Evaluation of the Large-Scale and Regional Climatic Response Across North Africa to Natural Variability in Oceanic Modes and Terrestrial Vegetation

Michael Notaro, Center for Climatic Research, University of Wisconsin-Madison
mnotaro@wisc.edu, (608) 261-1503

Fuyao Wang, Center for Climatic Research, University of Wisconsin-Madison

Yan Yu, Center for Climatic Research, University of Wisconsin-Madison

Jiafu Mao, Oak Ridge National Laboratory, Department of Energy

Xiaoying Shi, Oak Ridge National Laboratory, Department of Energy

Yaxing Wei, Oak Ridge National Laboratory, Department of Energy

Funding Source: Department of Energy Regional and Global Climate Modeling Program

Biogeochemistry Feedbacks Webinar, October 16, 2015

Study Region

The semi-arid Sahel represents the southern margin of the Saharan Desert and northern extent of the region affected by the boreal summer African monsoon. It is characterized by a strong meridional rainfall gradient, prolonged dry season, and intense JJAS rainy season with frequent organized convective disturbances (Rowell and Milford 1993; Poan et al. 2013).

Typically, the West African monsoon onset occurs in late June in conjunction with an abrupt northward push of the ITCZ (Sultan and Janicot 2000; Le Barbé et al. 2002), initiating the Sahel's wet season (Taylor 2008).

The Sahel exhibits pronounced rainfall variability on the intra-seasonal, interannual (e.g. linked to ENSO), and decadal time scales (Nicholson 1978, 1980; Brooks 2004; Janicot et al. 2011), with direct impacts on agriculture, human health, and the local economies (Sultan and Janicot 2003; Tarhule and Lamb 2003; Sultan et al. 2005).

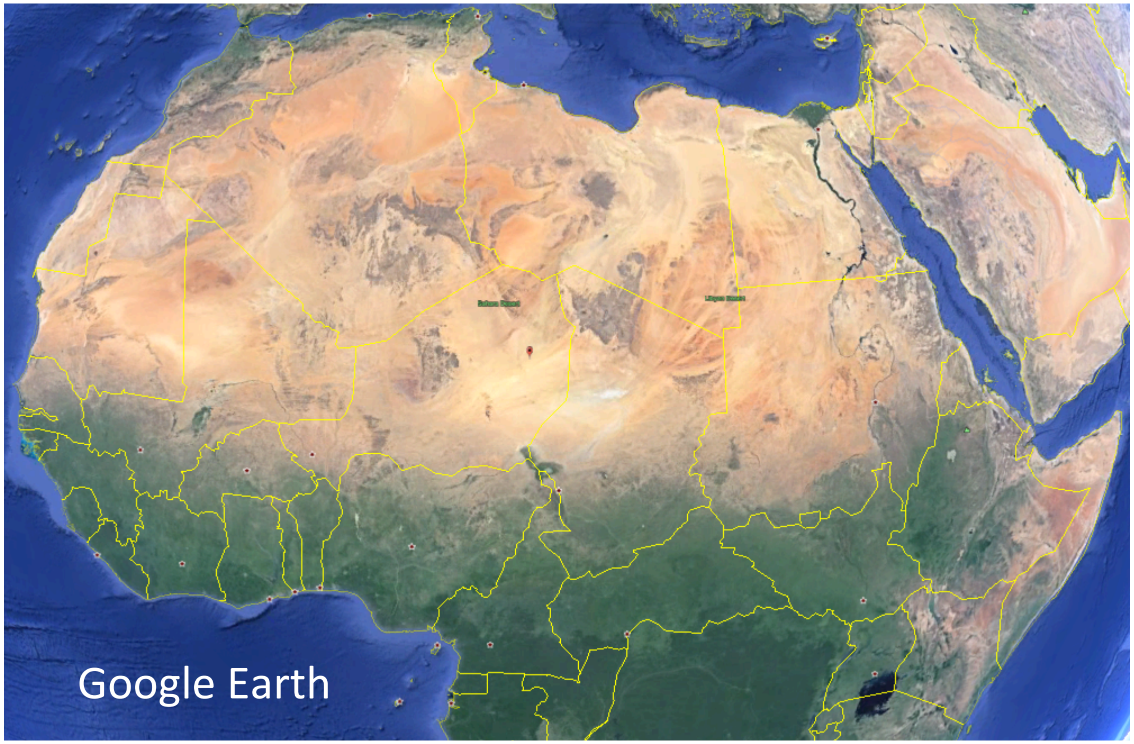

Study Region

Hydrologic extremes exhibit pronounced socio-economic impacts across the Sahel and Horn of Africa.

Roughly 1/3 of African people live within a drought-prone region (World Water Forum 2000), and drought events are often exacerbated by resulting health issues, including malaria and cholera (Few et al. 2004; Boko et al. 2007).

The 2011 drought across the Horn of Africa resulted in ≈ 50,000-100,000 deaths in Somalia, Ethiopia, and Kenya.

In contrast, extreme rainfall and flooding during 1997-1998 led to malaria epidemics in Kenya and Uganda (Kovats et al. 1999; Lindblade et al. 1999).

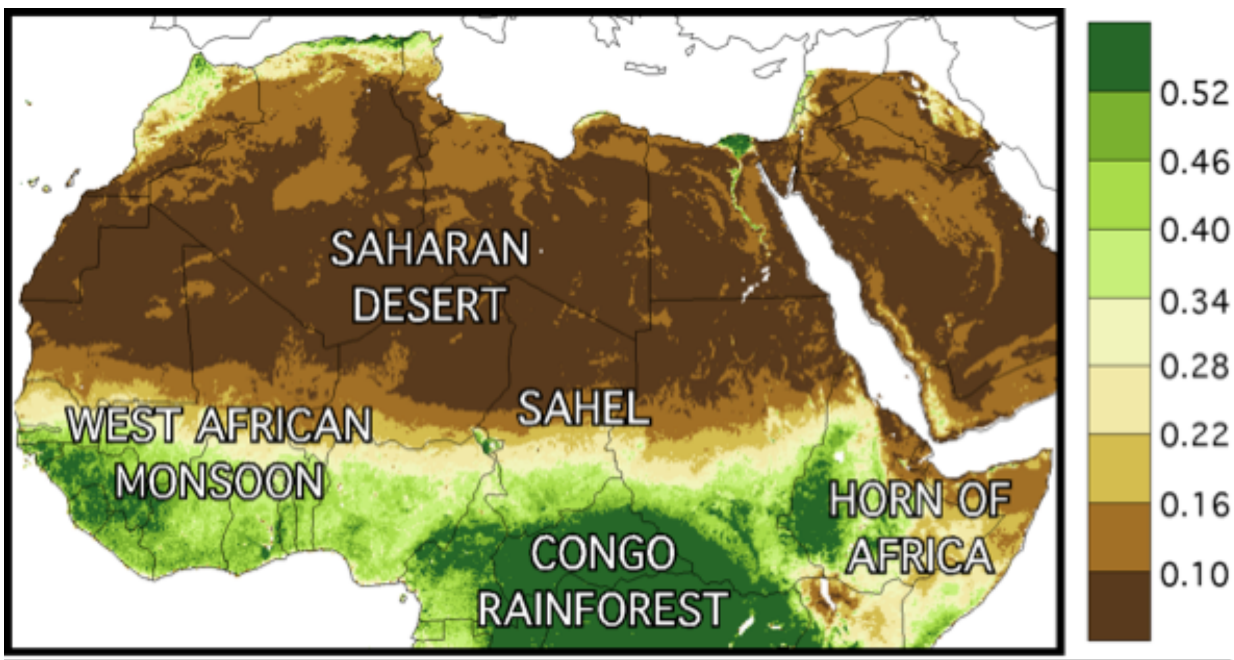

Annual mean Global Inventory Modeling and Mapping Studies (GIMMS) NDVI for 1982-2006 across North Africa. The seasonal cycle of NDVI is characterized as bimodal (two peaks) across the Congo, Horn of Africa, and the coast of the Gulf of Guinea and unimodal elsewhere.

Oceanic vs. Terrestrial Drivers of North African Rainfall

The Sahel's rainfall variability is characterized by both interannual and decadal variability (Farmer and Wigley 1985; Nicholson and Entekhabi 1986; Hulme 2001; Brooks 2004).

The Sahel experienced one of the most pronounced observed climatic shifts worldwide, as abundant rains during the 1950s-mid-1960s transitioned into extreme drought during the late 1960s-1990s (Lamb 1982; Katz and Glantz 1986; Lamb and Peppler 1992; Hulme 1996; Giannini et al. 2008a,b).

Much effort has been committed to attribute this recent multi-decadal drought to either oceanic drivers, namely regional or global SST anomalies (Folland et al. 1991; Rowell et al. 1995; Ward 1998; Giannini et al. 2003), or terrestrial drivers, specifically LULC changes and vegetation feedbacks (Charney 1975; Charney et al. 1977; Xue 1997; Zheng and Eltahir 1997; Clark et al. 2001; Taylor et al. 2002; Wang et al. 2004).

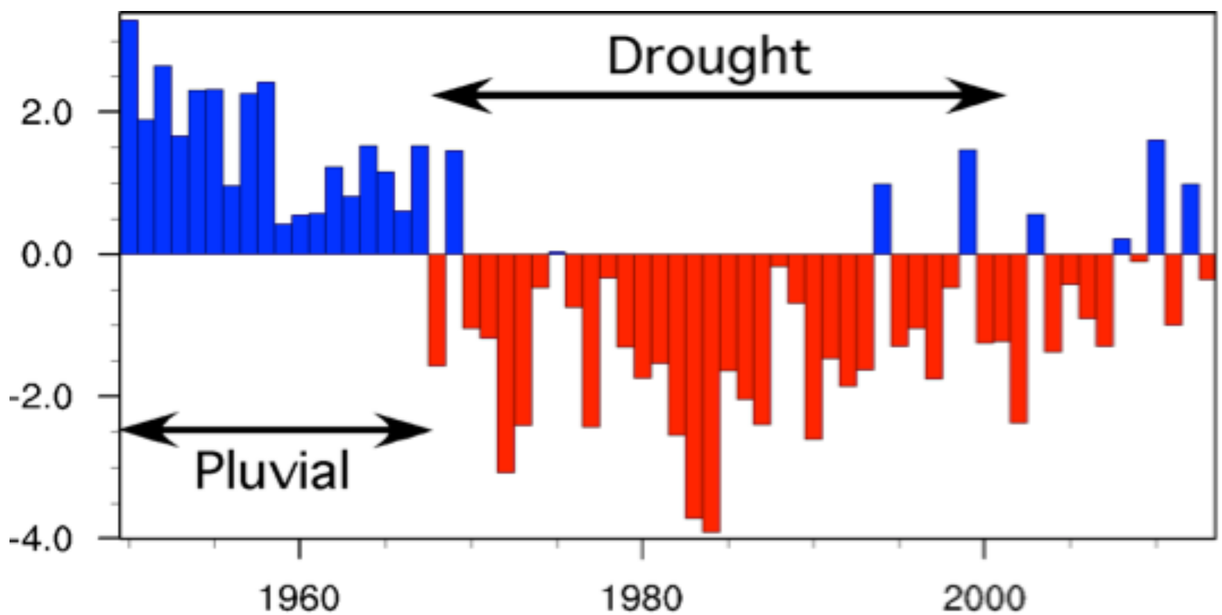

Time series of annual Sahel rainfall anomalies during 1950-2013 (data from JISAO, University of Washington). The Sahel rapidly transitioned from pluvial conditions during the 1950s-mid 1960s to drought during the late 1960s-1990s.

Oceanic vs. Terrestrial Drivers of North African Rainfall

Brooks (2004) and Lu and Delworth (2005) outlined competing arguments for the cause of the late 20th century Sahel drought, including external SST anomalies (Folland et al. 1986; Palmer 1986; Rowell et al. 1995) and local land degradation, desertification, and associated feedbacks (Charney 1975).

While Lu and Delworth (2005) and Hoerling et al. (2006) were generally able to reproduce the multi-decadal variability in Sahel rainfall in GCMs forced by observed SSTs alone, most modeling studies have concluded that Sahel rainfall variability is primarily driven by oceanic forcings and amplified by land-atmosphere interactions (Zeng et al. 1999; Giannini et al. 2003; Wang et al. 2004; Scaife et al. 2009; Kucharski et al. 2012).

Given uncertainty and inherent biases in GCMs, it is necessary to advance methodologies that can isolate the relative contributions of SST anomalies in oceanic basins and regional LAI anomalies toward driving Sahel rainfall in the observations, leading to an observational feedback benchmark against which models might be evaluated.

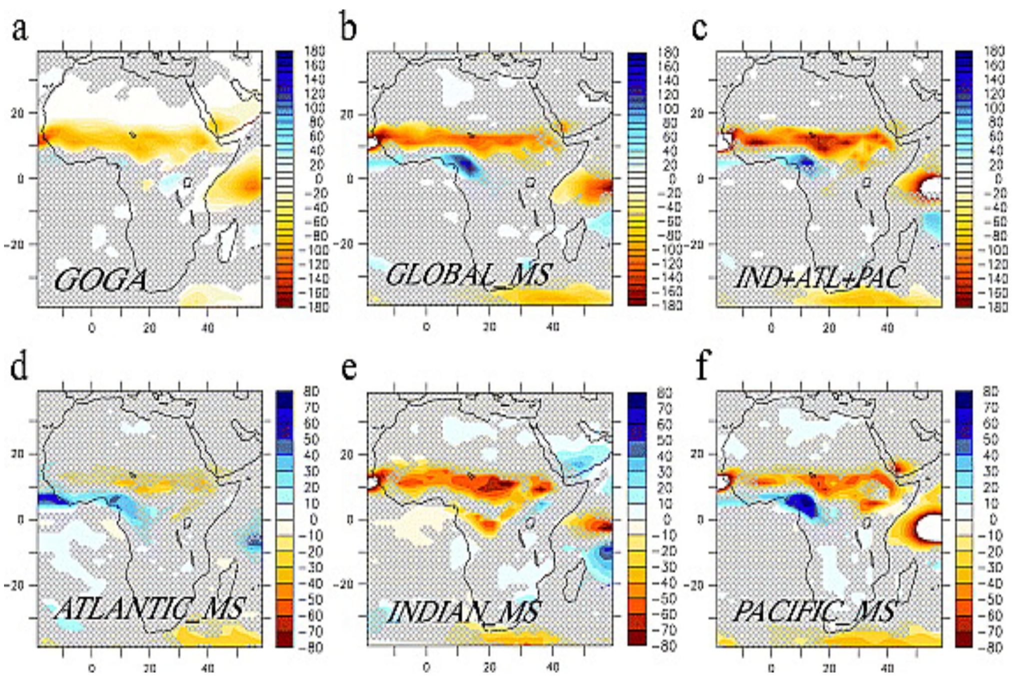

JAS rainfall response to SST forcing from different GFDL experiments (from Lu and Delworth 2005). All plots were scaled to correspond to 50-year trends (1950-2000), in mm/mon/50 years.

GOGA = prescribed global obs SST

INDIAN_MS = prescribed obs SST anomalies over Indian Ocean only

Indian/Pacific SST impacts > Atlantic SST impacts

Oceanic Drivers

While generally agreeing that tropical SST anomalies are critical drivers of Sahel rainfall, modeling studies have debated the relative contribution of tropical Atlantic, Indian, and Pacific SSTs and associated mechanisms (Giannini et al. 2003; Wang et al. 2004; Lu and Delworth 2005).

A number of uncertainties remain among these modeling studies of oceanic drivers of North African rainfall.

One glaring concern is that the model results are often inconsistent with each other. For instance, Lu and Delworth (2005) concluded that the Indian and Pacific Oceans largely regulate Sahel rainfall, with minimal contribution from the Atlantic Ocean, while Hoerling et al. (2006) simulated a strong influence from the Atlantic Ocean, with minimal contribution from the Indian Ocean.

The relative contribution of different oceanic basin forcings appears to change over time (Janicot et al. 1998).

These oceanic drivers can interact non-linearly (Janicot et al. 1998).

Due to the clear divergence in model-based findings, Lu and Delworth (2005) encouraged further investigations of the relative contribution of different tropical ocean basins in driving Sahel rainfall.

A deeper understanding of oceanic drivers of North African rainfall is needed from observational data so that regional climate predictability can be enhanced and climate models can be properly evaluated and improved.

Terrestrial Drivers

Vegetation and climate interact through a series of complex, poorly understood feedbacks, with the current understanding largely attributed to coupled vegetation-climate models (Notaro et al. 2006; Wang et al. 2014).

Vegetation impacts the climate directly through biophysical feedbacks, consisting of moisture, energy, and momentum exchanges with the atmosphere, and indirectly through biogeochemical processes that alter atmospheric CO_2 levels (Pielke et al. 1998; Bonan 2002).

Most studies on biophysical vegetation feedbacks have been restricted to running and analyzing coupled vegetation-climate model simulations.

However, climate models vary dramatically in terms of simulated land-atmosphere interactions (Liu et al. 2006), and few studies have attempted to validate simulated vegetation feedbacks against observations to give credibility to the findings (Notaro and Liu 2008; Wang et al. 2013, 2014).

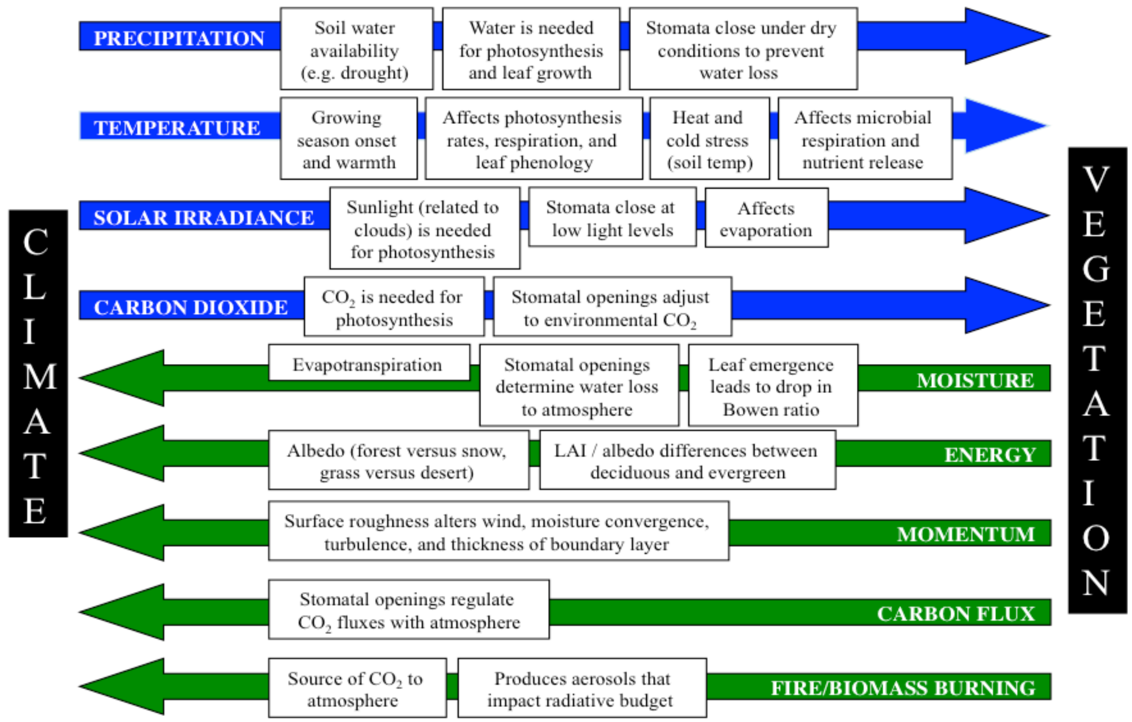

Schematic of vegetation-climate interactions (adapted from Notaro et al. 2006)

Terrestrial Drivers

Land-atmosphere interactions remain a key source of uncertainty in climate modeling and climate change projections (IPCC 2007).

While numerous modeling studies have explored vegetation feedbacks, their credibility is restricted by several key limitations (Wang et al. 2014).

Simulated feedbacks are model dependent, given that models largely differ in terms of their dynamical cores, numerical schemes, parameterizations, resolution, biases, and run lengths.

Nearly all modeling studies have applied extreme sensitivity experiments (e.g. complete replacement of a specific vegetation type with bare ground, either locally or globally). Such extreme experiments are unrealistic, since vegetation changes are typically heterogeneous and occur over time.

The vast majority of modeling studies have focused on the long-term climate equilibrium response to an imposed vegetation change, rather than the climatic response to intra-seasonal to interannual LAI variations, despite their importance to short-term climate prediction (Wang et al. 2013, 2014).

Owing to these modeling study limitations, observational studies of land surface feedbacks are critically needed (O'Brien 1986).

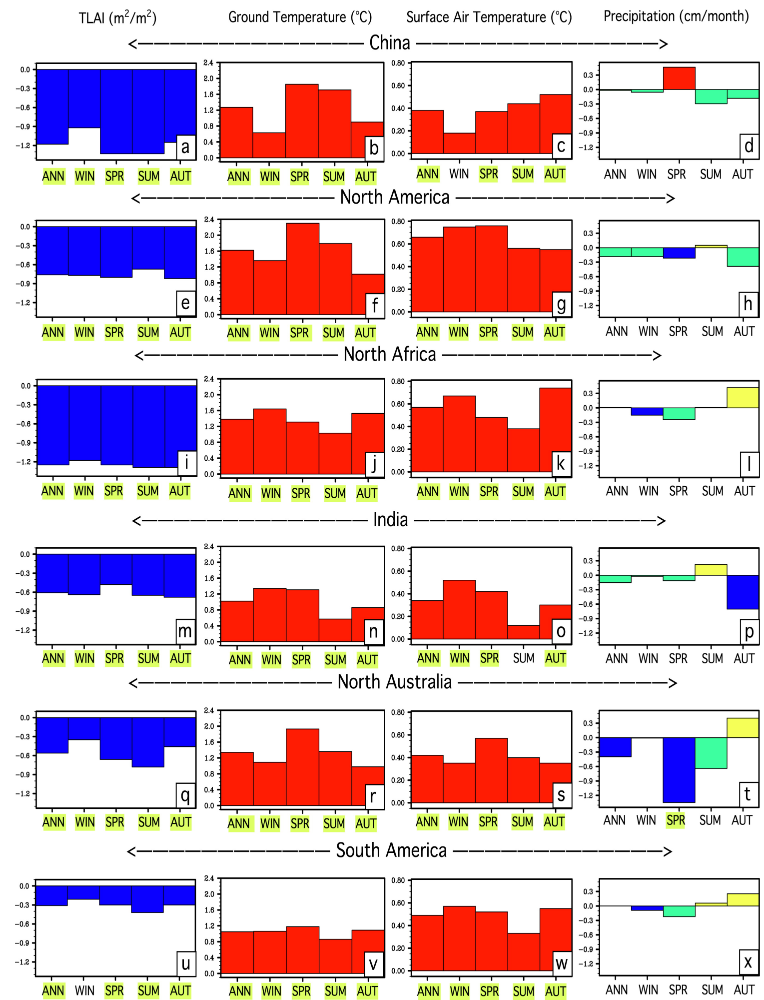

Annual/seasonal changes in LAI, ground and surface air temperature, and precipitation for 6 monsoon regions in response to an imposed vegetation cover reduction in CCSM3.5 (Notaro et al. 2011).

Development and Assessment of Generalized Equilibrium Feedback Assessment (GEFA)

To address the aforementioned challenges in extracting the impact of intra-annual to interannual variability in oceanic or terrestrial forcings on the atmosphere in the observational record, the multivariate statistical method, GEFA (Liu et al. 2008; Wen et al. 2010), was developed, based on the stochastic climate theory of Hasselmann (1976) and Frankignoul and Hasselmann (1977).

GEFA can extract the forcing of a slowly-evolving environmental variable (e.g. SST, LAI) on the rapidly-changing atmosphere, either in model output or observational data.

GEFA has been applied to examine the impacts of N. Pacific SST variability in CCSM3 (Zhong and Liu 2008), global SST variability on observed geopotential heights (Wen et al. 2010) and U.S. precipitation (Zhong et al. 2011), and oceanic and vegetation variability on N. American temperature and precipitation in observations and CCSM3.5 (Wang et al. 2013, 2014).

Several recent studies have explored GEFA's reliability in terms of quantifying the forcing of either SSTs or LAI on the atmosphere.

Development and Assessment of Generalized Equilibrium Feedback Assessment (GEFA)

Using a conceptual climate model, Liu et al. (2012a,b) demonstrated that GEFA produces consistent, and accurate, estimates of the atmospheric response to surface forcings (e.g. geopotential height response to ENSO or North Pacific modes) compared to linear inverse modeling (Penland and Sardeshmukh 1995a,b; Newman et al. 2009) and fluctuation-dissipation theorem (Leith 1975; Bell 1980).

Within CCSM3.5, Wang et al. (2013, 2014) performed dynamical ensemble experiments, with imposed anomalies of either basin SSTs or regional LAI within North America, and compared the atmospheric response to that predicted by statistical GEFA. Consistent feedback estimates between the independent statistical and dynamical approaches, in the same model, demonstrated GEFA's ability to isolate the impacts of SST anomalies in individual basins and separate the impact of land surface forcings from oceanic forcings. After validating GEFA in the model, the method was applied to observational data to assess controls on North America's climate and develop an observational feedback benchmark against which models may be assessed (Wang et al. 2013, 2014).

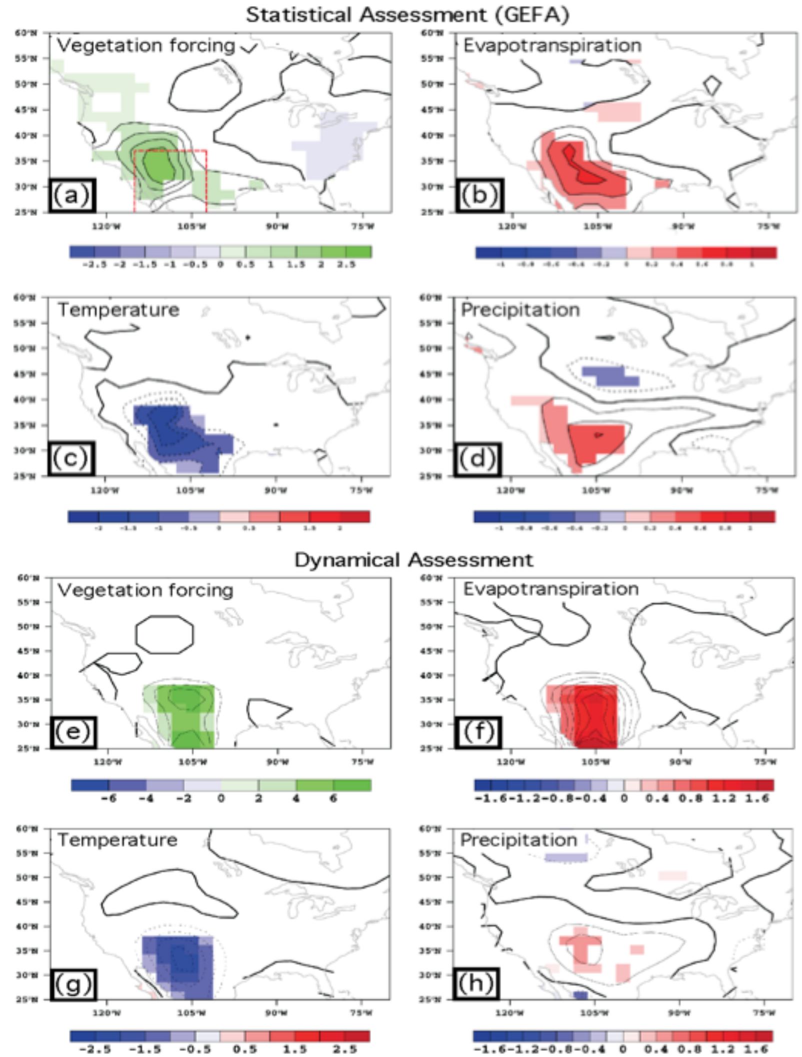

Impact of + LAI anomaly in N. American monsoon region on summer (b,f) ET (mm/day), (c,g) temperature (°C), and (d,h) rainfall (mm/day) in CCSM3.5, comparing (a-d) statistical (GEFA) and (e-h) dynamical assessments (Wang et al. 2014).

Summary of GEFA Methodology

An atmospheric variable (A) (e.g. precipitation) can be decomposed into 2 terms.

The first term is the feedback from a slowly-evolving variable (O) (e.g. SST, LAI) and the second is atmospheric internal noise (N).

The memory of the atmosphere (≈ 1 week) is shorter than that of SST or LAI (Notaro et al. 2006; Liu et al. 2006; Wang et al. 2013, 2014).

At time scales significantly longer than the atmospheric memory, the response of the atmospheric variable at time t, A(t), to the oceanic or land surface variable, O(t), is the feedback coefficient, B, given as (Frankignoul et al. 1998): $A(t) = BO(t) + N(t)$.

Right multiplying $O^T(t-\tau)$ on both sides of this equation and applying the covariance yield:
$C_{AO}(\tau) = BC_{OO}(\tau) + C_{NO}(\tau)$.

τ is the time scale, exceeding the atmospheric adjustment time, C is a covariance matrix, superscript "T" indicates a transpose, and L is the time series' length.

The lagged covariance matrices are as follows:
$C_{AO}(\tau) = {}^1/_L\, A(t)O^T(t-\tau)$ $\quad C_{OO}(\tau) = {}^1/_L\, O(t)O^T(t-\tau)$ $\quad C_{NO}(\tau) = {}^1/_L\, N(t)O^T(t-\tau)$

Oceanic or vegetation variability cannot be forced by atmospheric internal noise at a later time, so $C_{NO}(\tau)=0$. As a result, the feedback matrix can be computed as: $B = C_{AO}(\tau)\, C_{OO}^{-1}(\tau)$

The estimated feedback matrix represents the *instantaneous* influence of a slowly-evolving variable (e.g. SST, LAI) on an atmospheric variable.

Summary of GEFA Methodology

An effective method to reduce sampling error, due to high correlation among forcing fields (Wen et al. 2010), is to perform GEFA in truncated SST empirical orthogonal function (EOF) space.

Wang et al. (2013, 2014) and Wen et al. (2010) divided the global ocean into 5 non-overlapping ocean basins: the tropical Pacific (TP), North Pacific (NP), tropical Indian (TI), tropical Atlantic (TA), and North Atlantic (NA).

In the ocean feedback study of Wang et al. (2013), the first 2 principal components of each of the 5 ocean basins were combined into a single forcing matrix: O = [TP1 TP2 NP1 NP2 TI1 TI2 TA1 TA2 NA1 NA2].

For example, TP1 represented the first PC of tropical Pacific SSTs.

Wang et al. (2014) expanded the analysis of North American climate beyond oceanic forcings to include vegetation in the forcing matrix, namely remotely-sensed NDVI averaged over the North American monsoon region (NAMR).

After normalizing the ocean and vegetation terms, the forcing matrix became:
O = [NAMR TP1 TP2 NP NP2 TI1 TI2 TA1 TA2 NA1 NA2].

GEFA can therefore reveal the local and remote impacts of interannual variability in each individual oceanic and terrestrial forcing on the atmosphere.

Key Questions

(1) Is the multivariate statistical tool, GEFA, capable of accurately separating feedbacks induced by variability across individual oceanic basins and terrestrial ecoregions in North Africa?

(2) What are the primary natural modes of variability, within the oceanic and terrestrial components of the Earth system which regulate the observed regional climate of North Africa? How important are vegetation biophysical feedbacks in modulating the observed seasonal climate of North Africa, including the West African monsoon?

(3) How well do CMIP5 models capture large-scale and regional-scale responses across North Africa to natural variability in oceanic modes and vegetation, compared to the observed GEFA benchmark?

(4) How will North African land-ocean-atmosphere feedbacks be altered by anthropogenic climate change?

Objectives

(1) GEFA's reliability in diagnosing oceanic and terrestrial feedbacks to the atmosphere across North Africa will be assessed in CESM using dynamical sensitivity experiments. Consistent feedback estimates from the independent statistical (GEFA) and dynamical methods, employed in the same climate model, will demonstrate GEFA's credibility, so that it can be confidently applied to observations and CMIP5 models.

(2) GEFA will be applied to observational, remote sensing, and reanalysis data to identify, and explore the mechanism behind, the primary natural modes of variability in global oceanic modes and regional LAI that regulate sub-seasonal to interannual variations in North African climate.

(3) The CMIP5 models' ability to represent large-scale and regional-scale responses to dominant oceanic and terrestrial modes of variability for North Africa will be evaluated using GEFA, leading to the creation of performance metrics to aid in model intercomparison and development.

(4) Since anthropogenic climate change may alter the seasonality and intensity of land-ocean-atmosphere feedbacks, GEFA will also be applied to CMIP5 simulations for the 21st century and beyond.

GENERAL METHODOLOGY

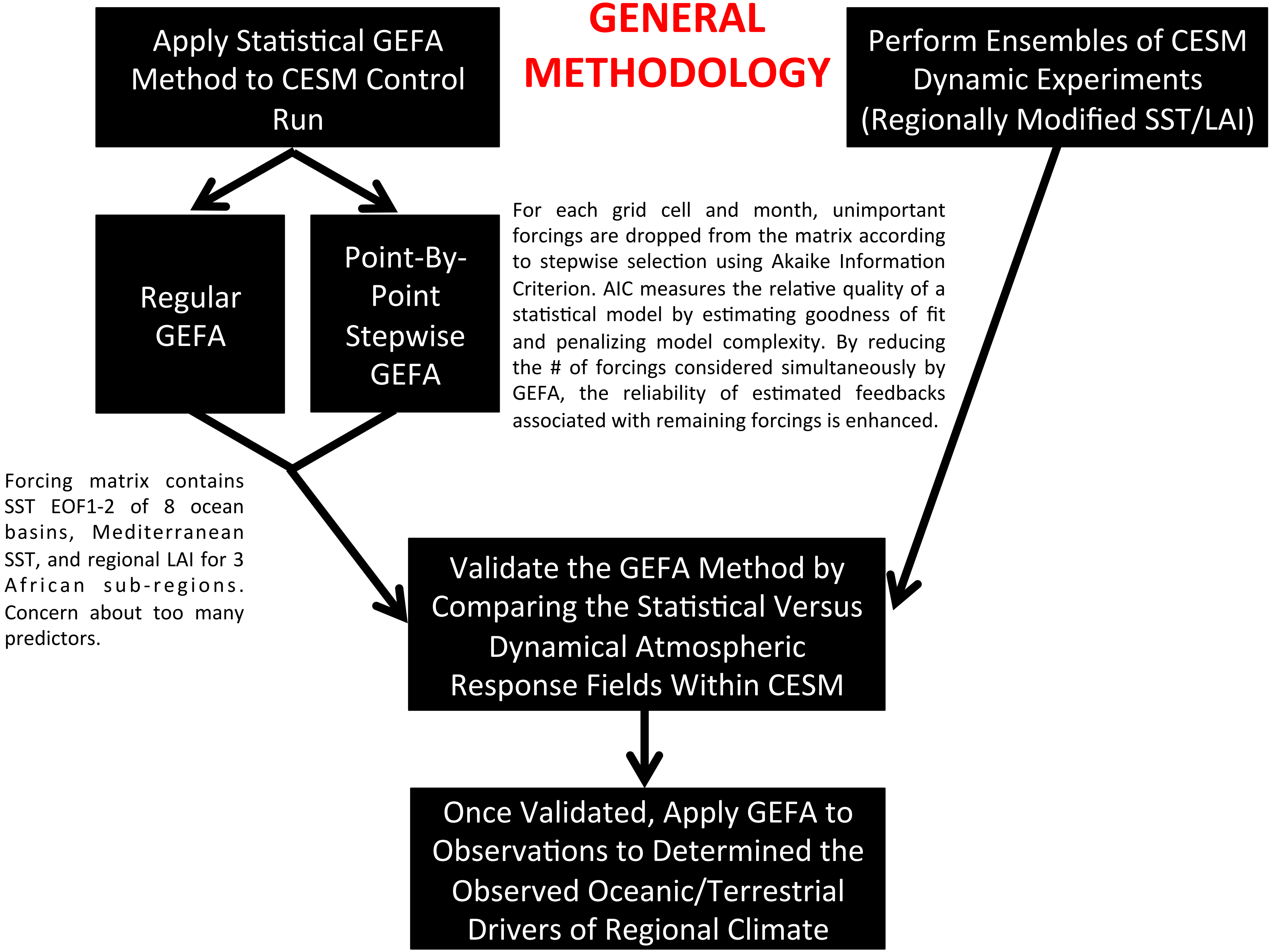

Generation of CESM Control Run

Step 1. The offline carbon-nitrogen dynamic vegetation (CNDV) model was spun up for 2050 years. At that point, it was considered in equilibrium, as the globally-averaged absolute value of terrestrial Net Ecosystem Exchange (NEE) was less than 0.05 PgC yr^{-1} (Hoffman et al. 2008). This offline simulation generated the initial land surface file of plant functional type (PFT) distribution and terrestrial carbon pools for initializing the fully coupled CESM.

Step 2. Using the resulting CNDV file of PFT distribution and carbon pools, the fully coupled 0.9° x 1.25° CESM control run was produced, with 100 years of spin up followed by 300 years of simulation for analysis. The control run would be used to evaluate the reliability of GEFA over North Africa.

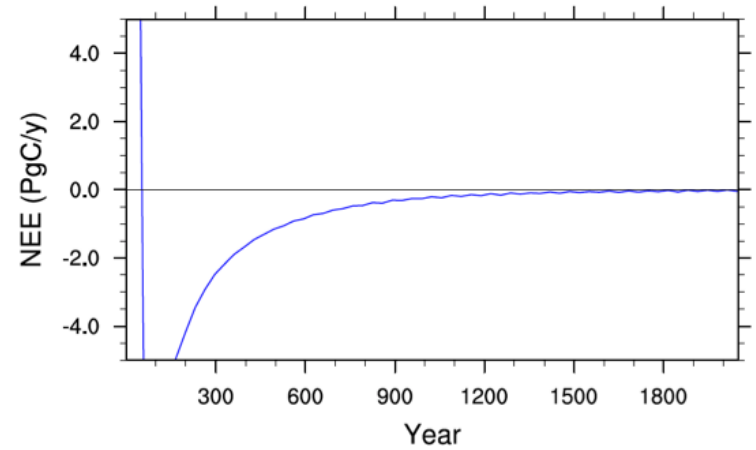

Time series of globally-averaged monthly land NEE from the offline CNDV run. Negative NEE indicates a growing carbon sink from the atmosphere into the land. By year 2040, the absolute value of NEE was less than 0.05 PgC $year^{-1}$, indicating that the terrestrial carbon pools were roughly in equilibrium.

Evaluation of CESM Control Run: SSTs

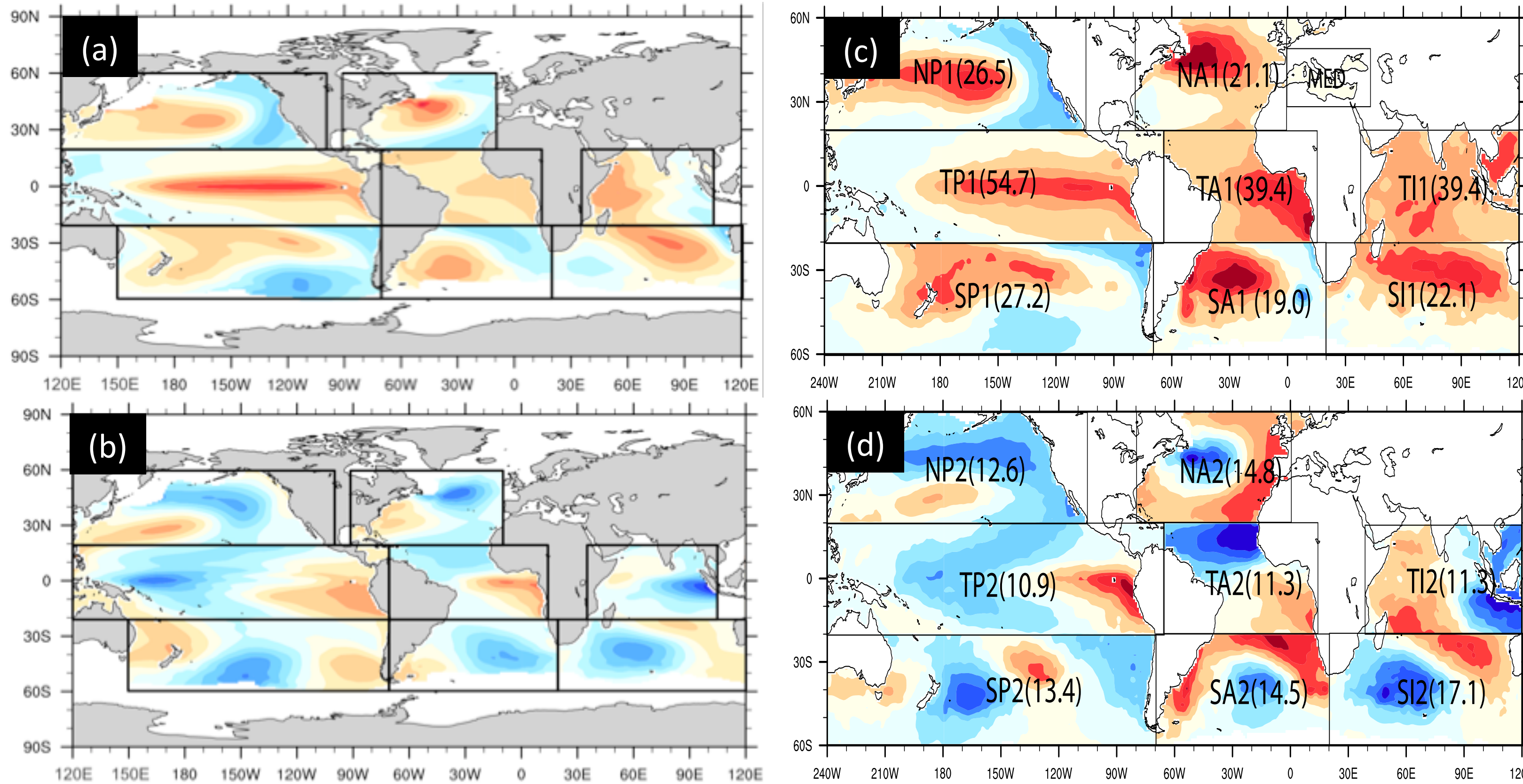

Spatial patterns associated with (a) 1st and (b) 2nd leading EOF modes of SSTs in the **CESM control run** within 8 ocean basins (N. Pacific, tropical Pacific, S. Pacific, N. Atlantic, tropical Atlantic, S. Atlantic, tropical Indian, and S. Indian).

Spatial patterns associated with (c) 1st and (d) 2nd leading EOF modes of **observed** SSTs within 8 ocean basins, using the Hadley Centre Global Sea Ice Coverage and SST dataset for 1900-2011.

The performance of CESM was evaluated in terms of simulated spatial and temporal patterns in global SSTs. CESM is applied in our study as a modeling tool to investigate the credibility of GEFA, by comparing statistically-assessed ocean-land-atmosphere feedbacks using GEFA against dynamically-assessed feedbacks using ensemble experiments. Therefore, exceptional model performance compared to observations is not a necessity.

Evaluation of CESM Control Run: SSTs

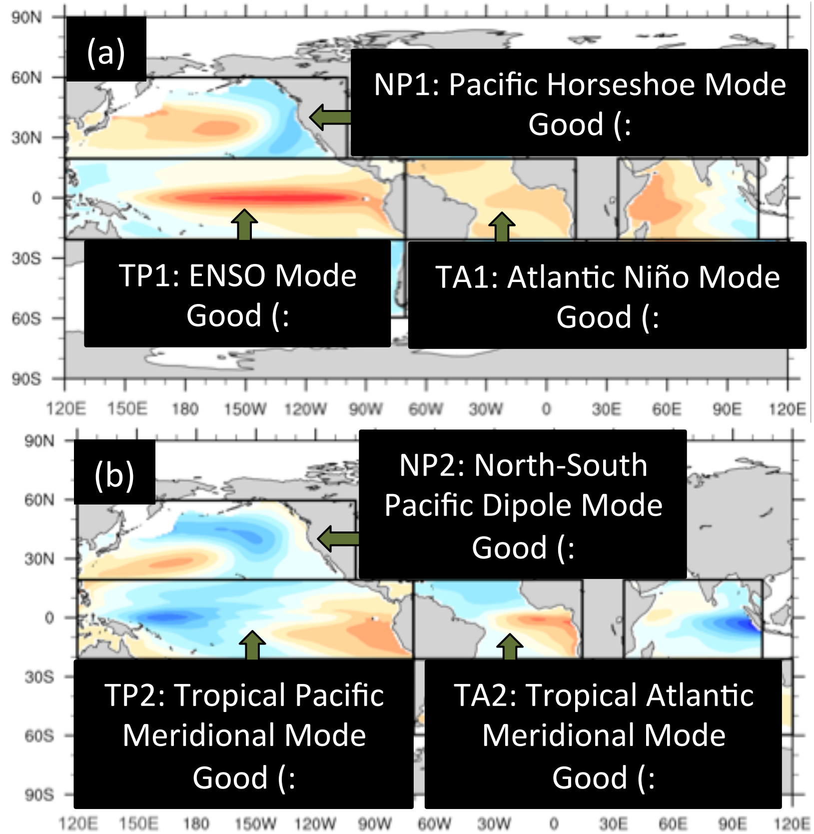

Spatial patterns associated with (a) 1st and (b) 2nd leading EOF modes of SSTs in the **CESM control run** within 8 ocean basins (N. Pacific, tropical Pacific, S. Pacific, N. Atlantic, tropical Atlantic, S. Atlantic, tropical Indian, and S. Indian).

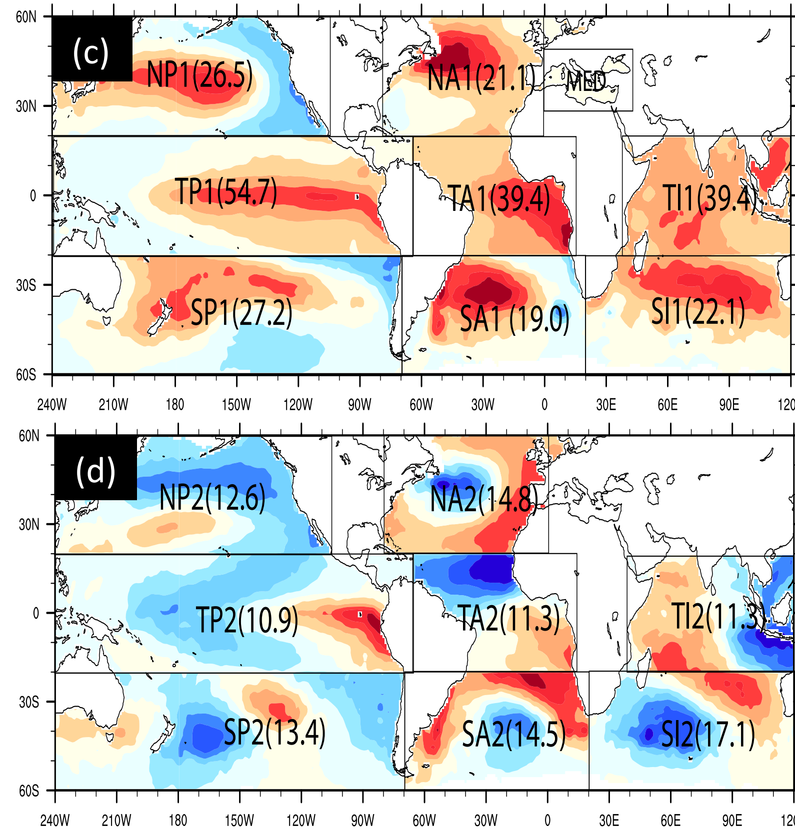

Spatial patterns associated with (c) 1st and (d) 2nd leading EOF modes of **observed** SSTs within 8 ocean basins, using the Hadley Centre Global Sea Ice Coverage and SST dataset for 1900-2011.

The performance of CESM was evaluated in terms of simulated spatial and temporal patterns in global SSTs. CESM is applied in our study as a modeling tool to investigate the credibility of GEFA, by comparing statistically-assessed ocean-land-atmosphere feedbacks using GEFA against dynamically-assessed feedbacks using ensemble experiments. Therefore, exceptional model performance compared to observations is not a necessity.

Evaluation of CESM Control Run: SSTs

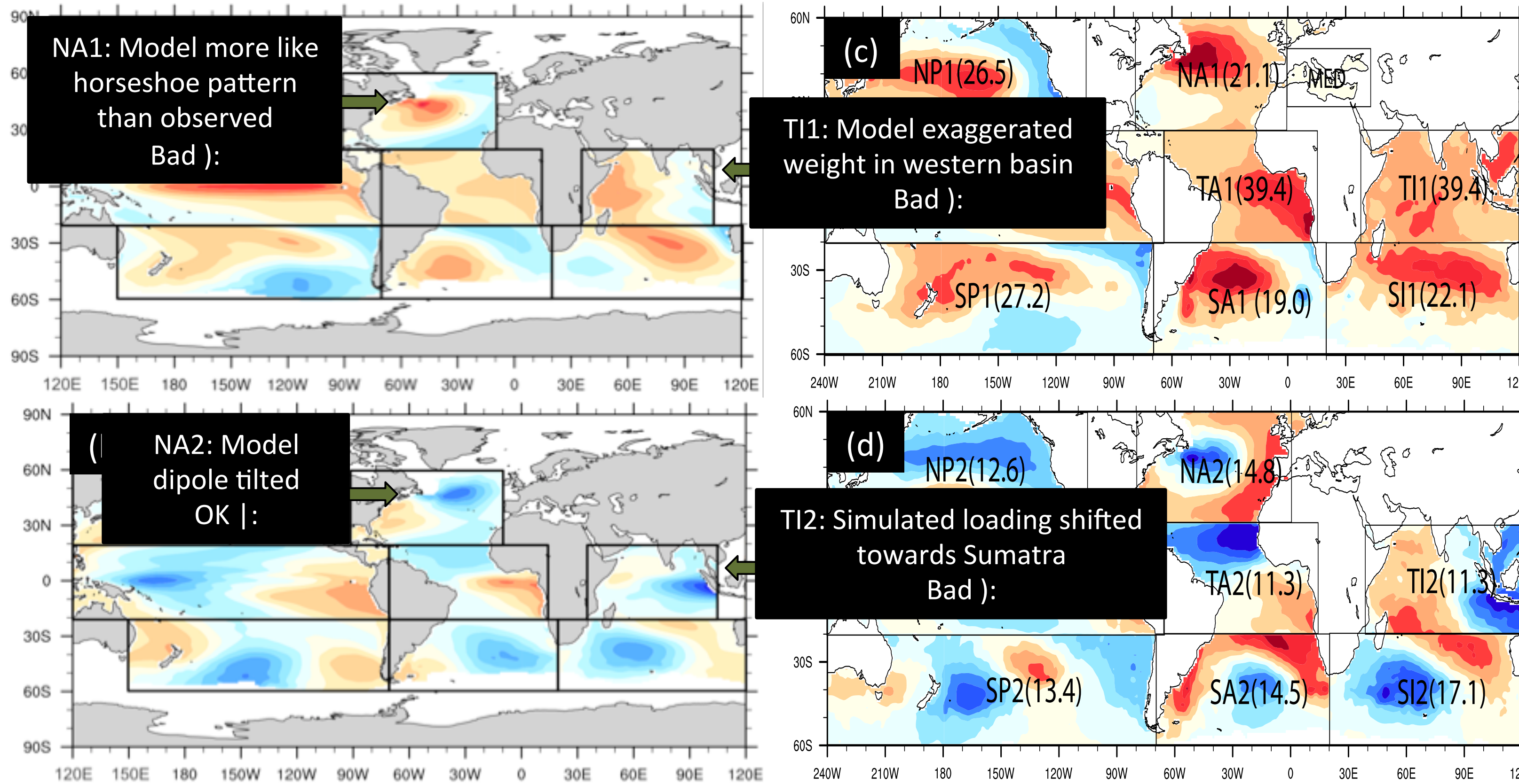

Spatial patterns associated with (a) 1st and (b) 2nd leading EOF modes of SSTs in the **CESM control run** within 8 ocean basins (N. Pacific, tropical Pacific, S. Pacific, N. Atlantic, tropical Atlantic, S. Atlantic, tropical Indian, and S. Indian).

Spatial patterns associated with (c) 1st and (d) 2nd leading EOF modes of **observed** SSTs within 8 ocean basins, using the Hadley Centre Global Sea Ice Coverage and SST dataset for 1900-2011.

The performance of CESM was evaluated in terms of simulated spatial and temporal patterns in global SSTs. CESM is applied in our study as a modeling tool to investigate the credibility of GEFA, by comparing statistically-assessed ocean-land-atmosphere feedbacks using GEFA against dynamically-assessed feedbacks using ensemble experiments. Therefore, exceptional model performance compared to observations is not a necessity.

Evaluation of CESM Control Run: Precipitation

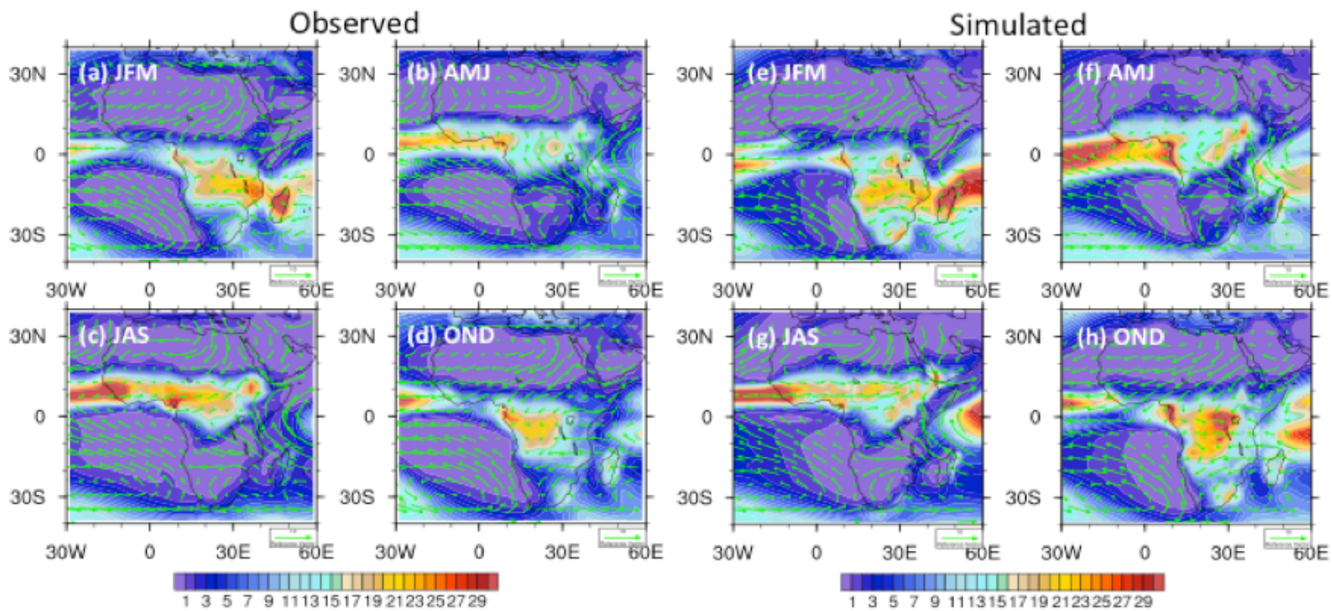

Spatial pattern of mean precipitation (shaded, cm month^{-1}) and 850-hPa wind by season from (a-d) GPCP and ERA-Interim and (e-h) CESM control run.

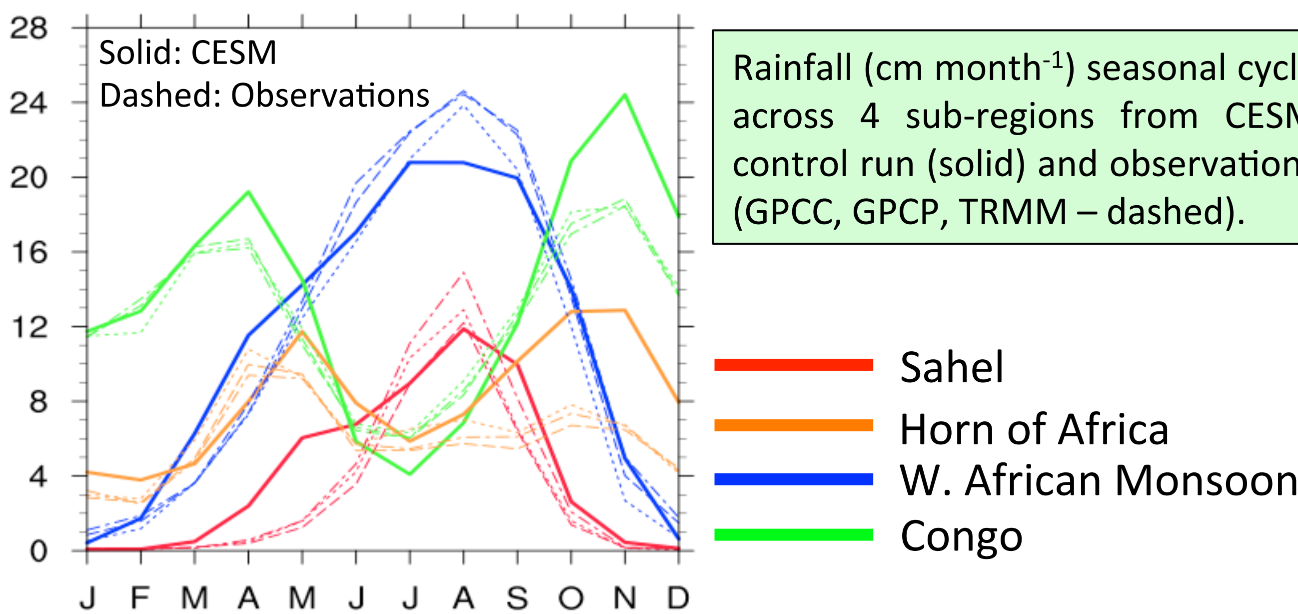

Rainfall (cm month^{-1}) seasonal cycle across 4 sub-regions from CESM control run (solid) and observations (GPCC, GPCP, TRMM – dashed).

The simulated North African precipitation climatology was compared against GPCC, GPCP, and TRMM.

CESM generally reproduced the observed seasonal timing and magnitude of rainfall, including the observed single peak over the Sahel and W. African monsoon region and dual peak over the Congo (related to ITCZ), although with a prolonged simulated rainy season in the monsoon region and Sahel.

Compared to observations, simulated rainfall was generally too low during JJA and too great during MAM and SON (including the short-rains in Horn of Africa).

Generation of CESM Dynamic Experiments

In order to evaluate the performance of GEFA, we created ensembles of data-ocean / data-ice CESM dynamical experiments.

Consistent response fields between the (1) application of the statistical GEFA approach to the CESM control run and the (2) CESM dynamical experiments (imposed SST anomalies in a given ocean basin) for a given oceanic mode demonstrate GEFA's reliability.

For each oceanic mode, 20 ensemble members are produced with a + phase and 20 members are produced with a - phase of that basin's SST EOF pattern.

So far, ensembles have been produced for SST EOF1 of the topical Pacific (TP1), tropical Indian (TI1), and tropical Atlantic (TA1).

Global SSTs are fixed to the mean seasonal cycle of the control run, except over the focal ocean basin, in which SSTs are assigned anomalies based on +/- phase of its EOF pattern.

The linear response to a given oceanic mode is determined by (P-N)/2, in which P is the mean response to + phase and N is the mean response to – phase. This is compared to GEFA results, as GEFA is a linear statistical method.

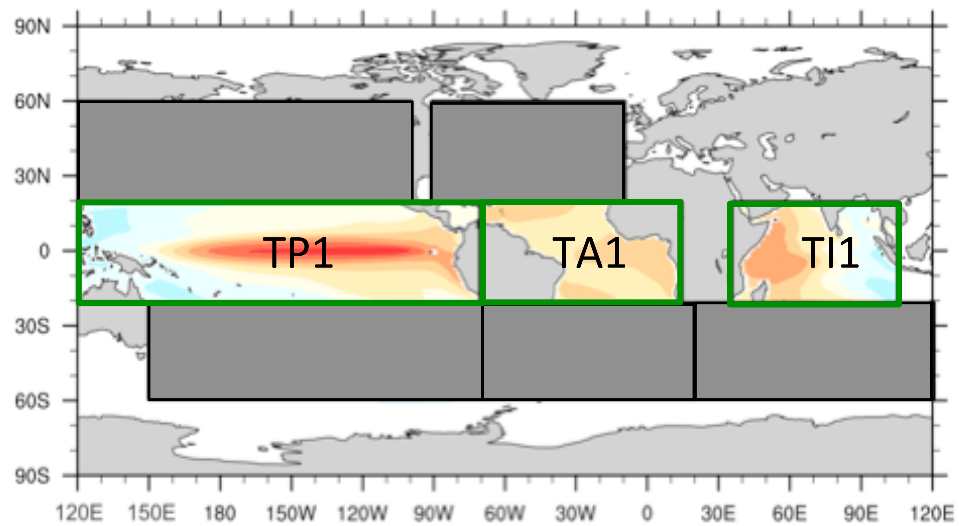

Sensitivity of GEFA to Record Length

Spatial Correlation | Root Mean Square Diff | Fraction of Area With Consistent Sign

Tropical Pacific SST EOF1 (TP1)

Tropical Atlantic SST EOF1 (TA1)

Tropical Indian SST EOF1 (TI1)

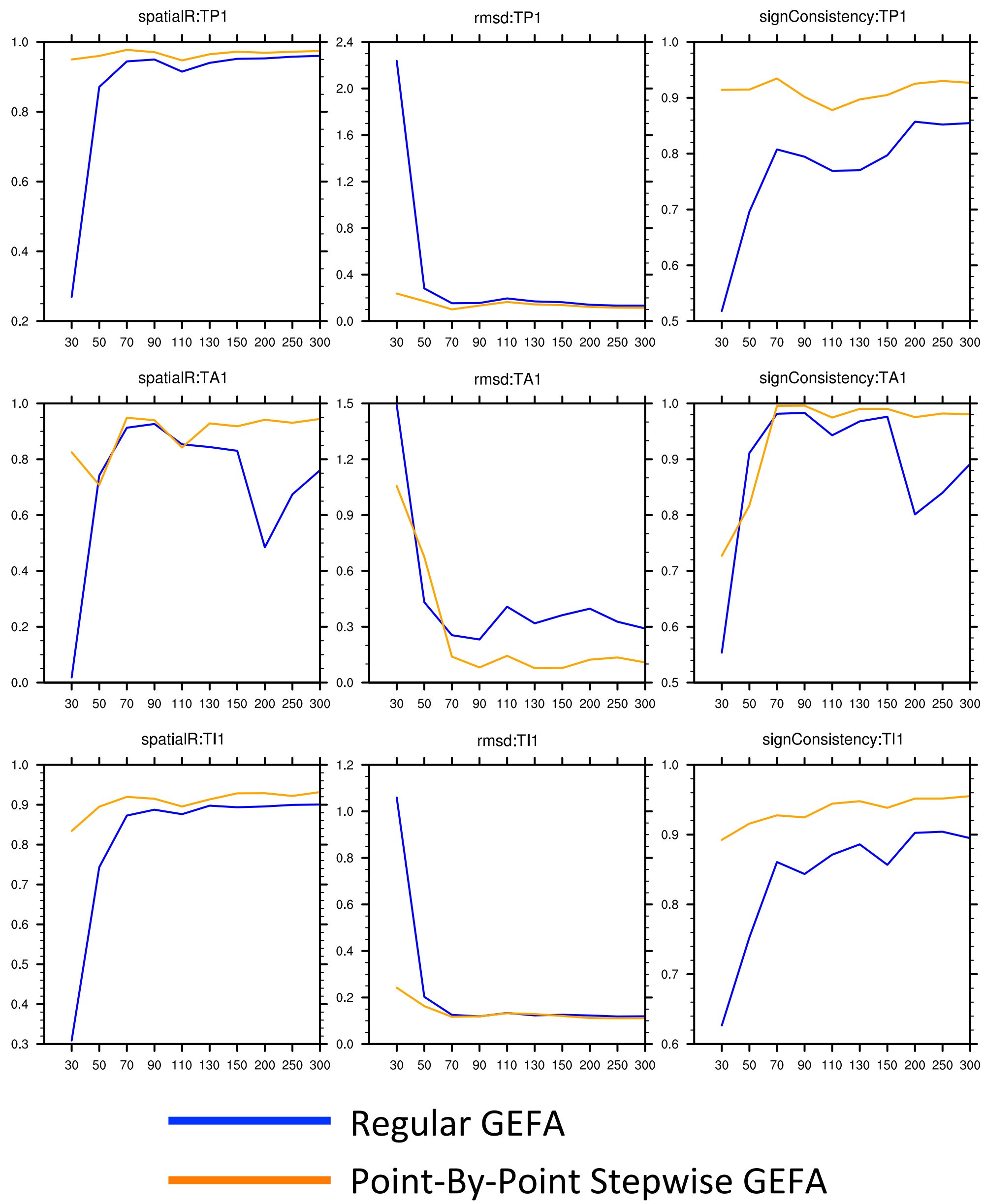

Comparison between GEFA (both regular and point-by-point stepwise GEFA), applied to varying #s of years from the CESM control run, and CESM dynamical experiments in terms of the **global response in November air temperature** to TP1, TA1, and TI1.

GEFA-based response fields to oceanic forcings stabilize with increasing record lengths, with the signal emerging over the noise.

Point-by-point stepwise GEFA yields more reliable response fields to oceanic forcings than regular GEFA, especially for short time records. This is critical when we apply GEFA to the short observational record.

Sensitivity of GEFA to Record Length

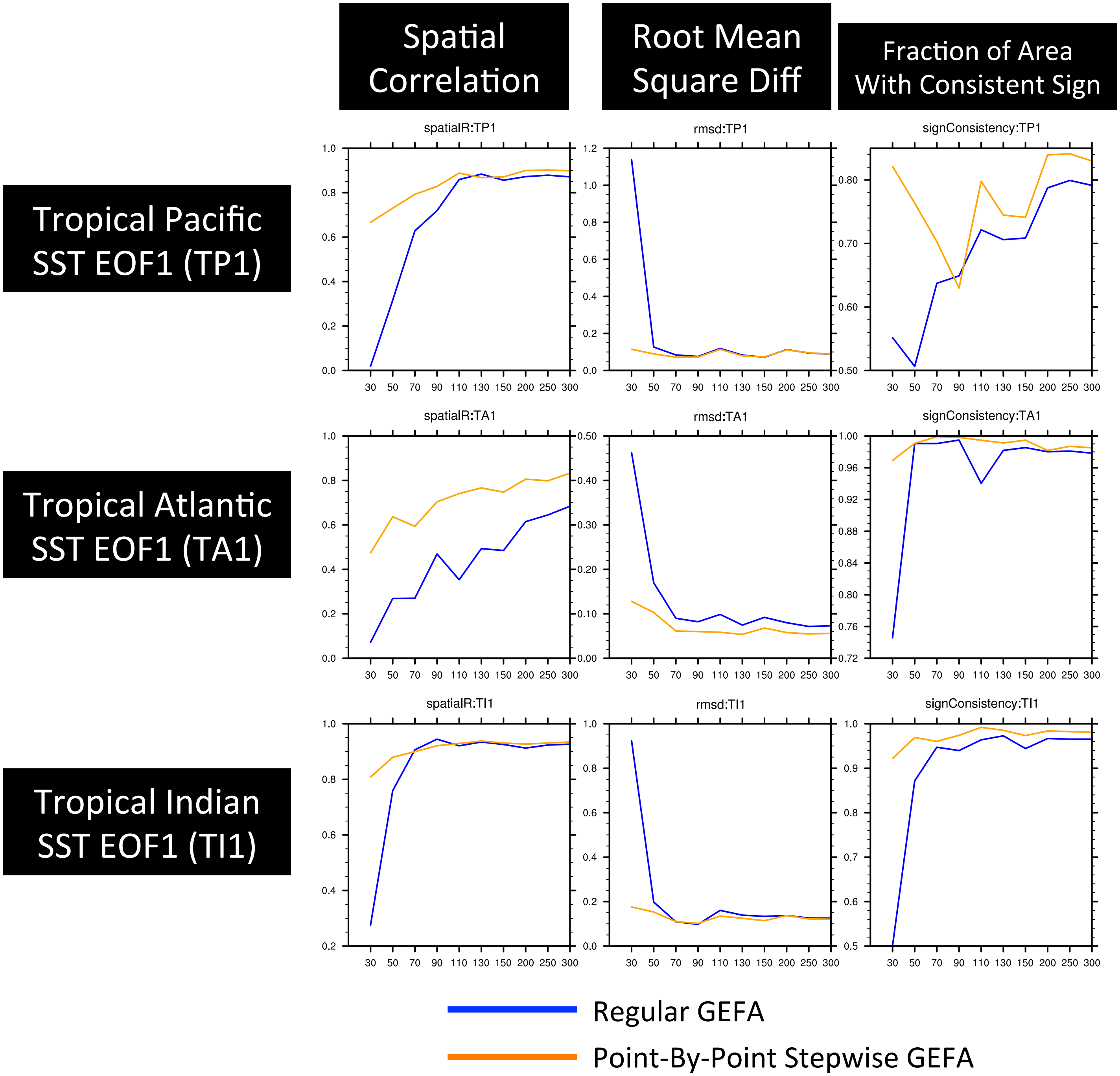

Comparison between GEFA (both regular and point-by-point stepwise GEFA), applied to varying #s of years from the CESM control run, and CESM dynamical experiments in terms of the **North African response in November air temperature** to TP1, TA1, and TI1.

Sensitivity of GEFA to Record Length

Comparison between GEFA (both regular and point-by-point stepwise GEFA), applied to varying #s of years from the CESM control run, and CESM dynamical experiments in terms of the **global response in July precipitation** to TP1, TA1, and TI1.

	Spatial Correlation	Root Mean Square Diff	Fraction of Area With Consistent Sign
Tropical Pacific SST EOF1 (TP1)			
Tropical Atlantic SST EOF1 (TA1)			
Tropical Indian SST EOF1 (TI1)			

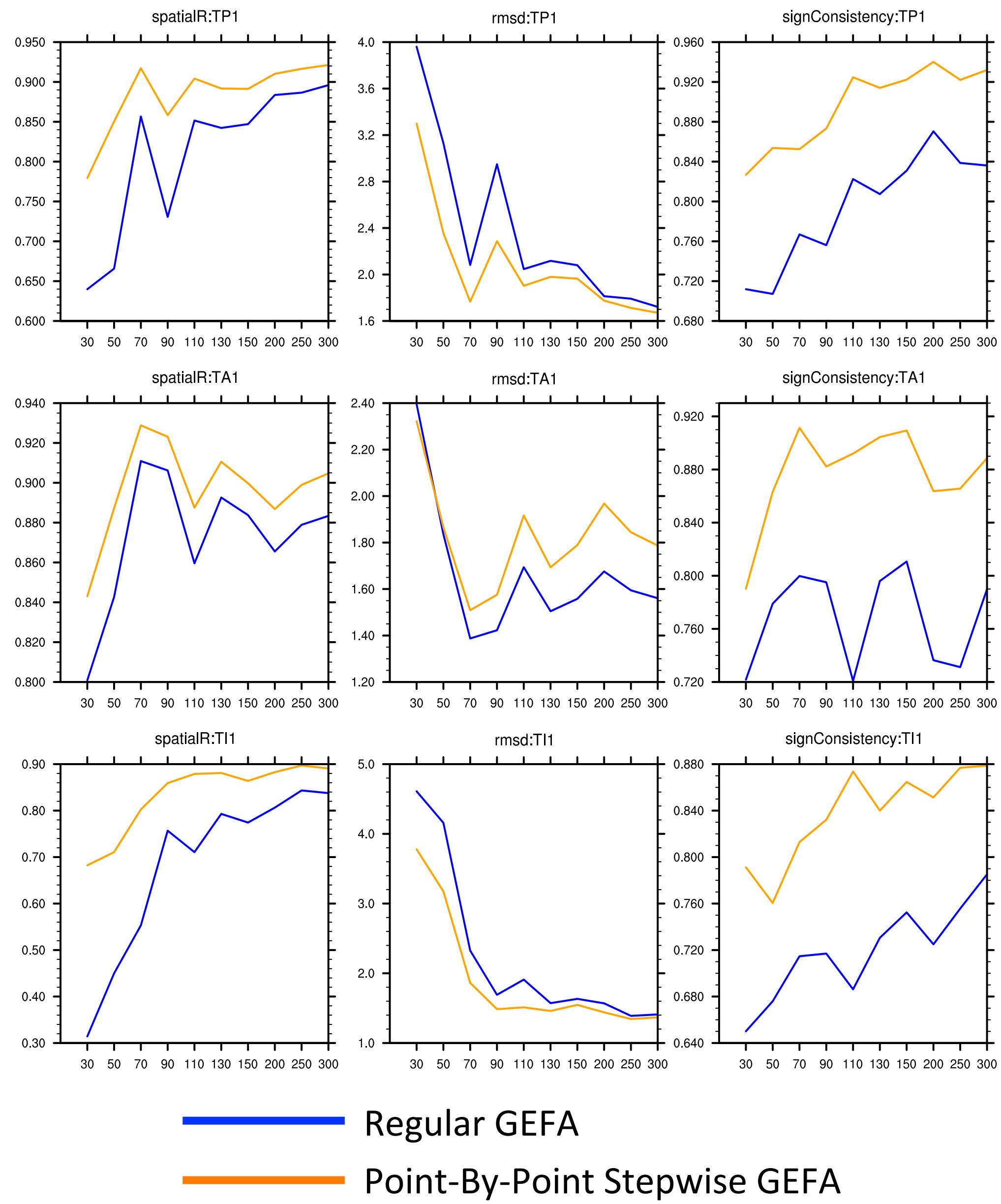

Sensitivity of GEFA to Record Length

	Spatial Correlation	Root Mean Square Diff	Fraction of Area With Consistent Sign
Tropical Pacific SST EOF1 (TP1)			
Tropical Atlantic SST EOF1 (TA1)			
Tropical Indian SST EOF1 (TI1)			

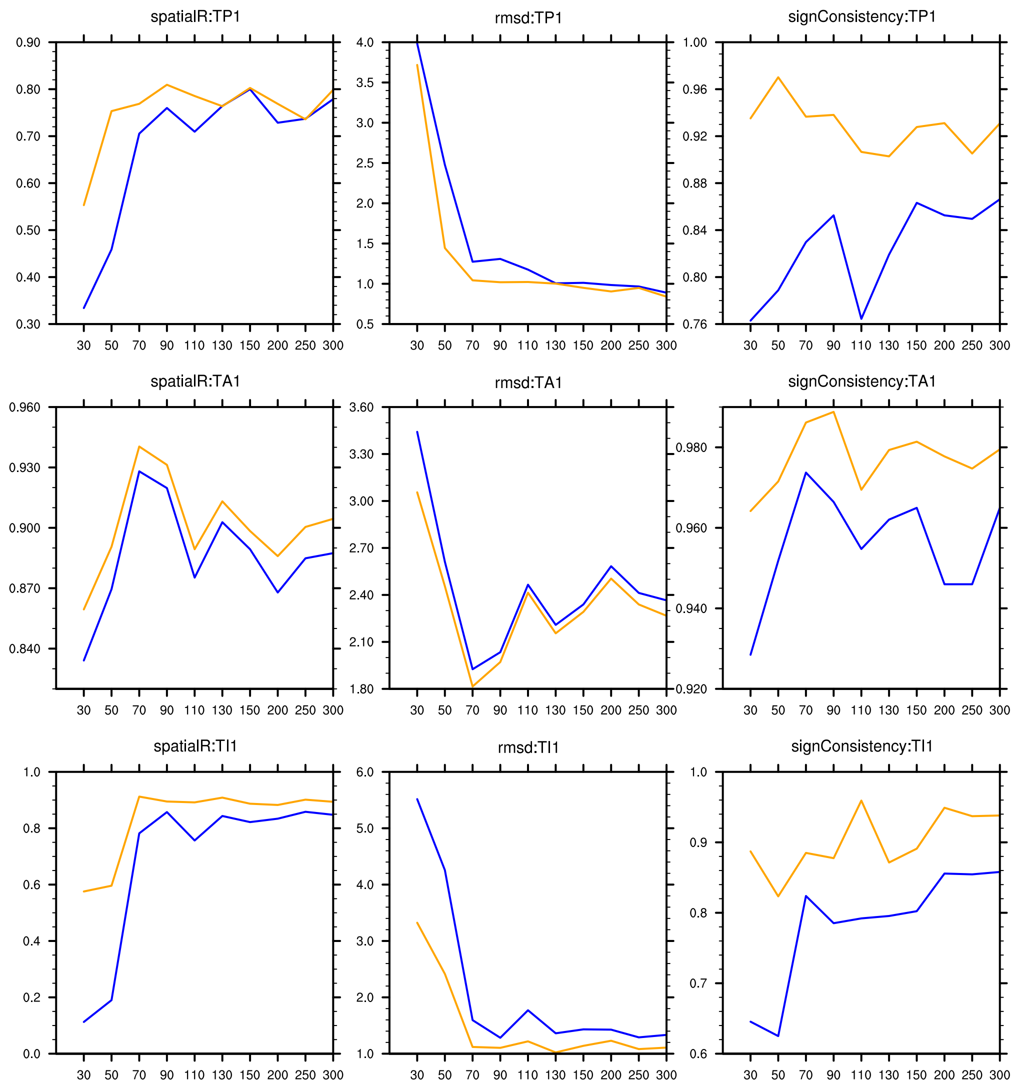

Regular GEFA

Point-By-Point Stepwise GEFA

Comparison between GEFA (both regular and point-by-point stepwise GEFA), applied to varying #s of years from the CESM control run, and CESM dynamical experiments in terms of the **North African response in July precipitation** to TP1, TA1, and TI1.

Evaluation of GEFA

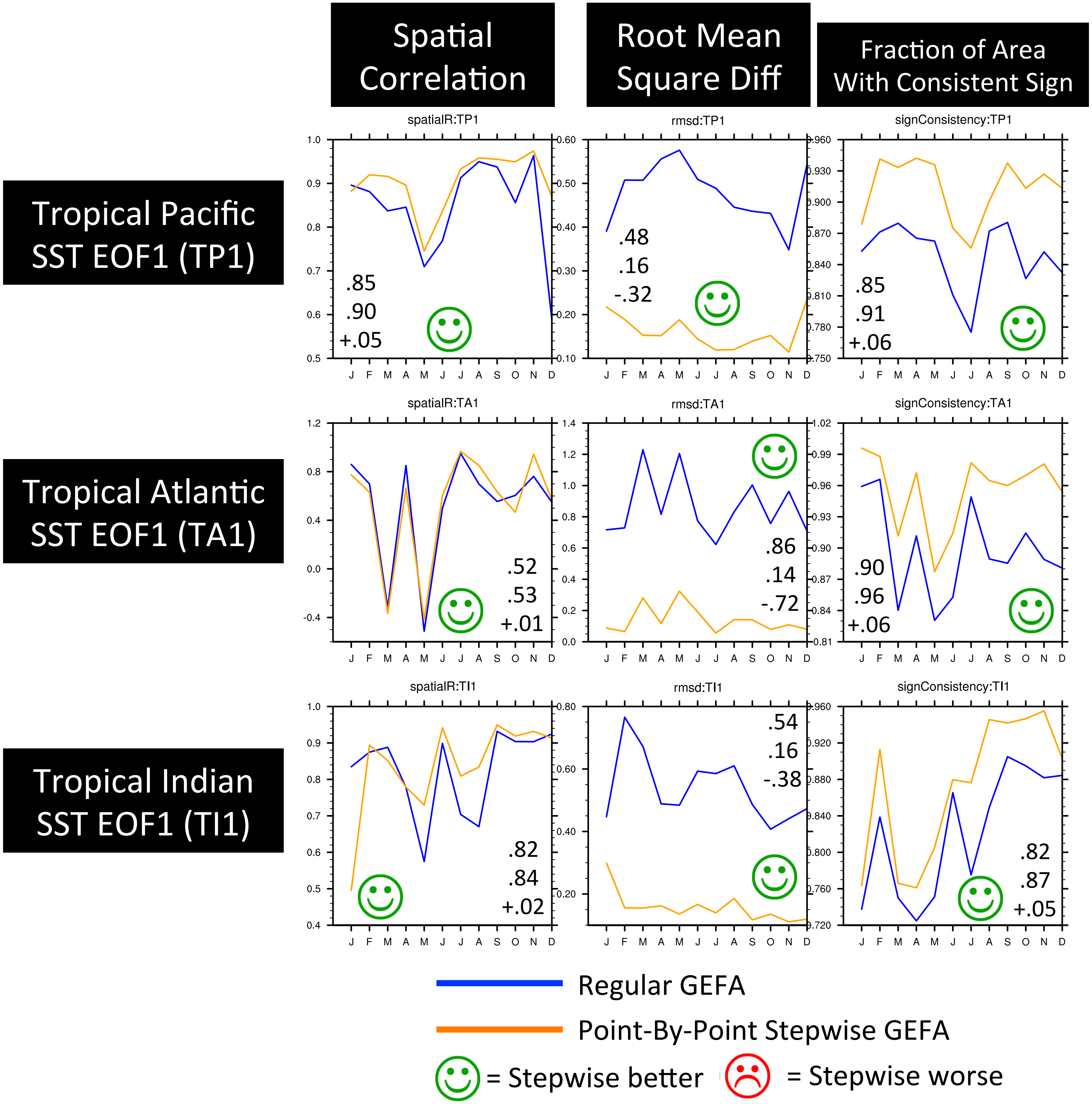

Comparison between statistical GEFA (both regular and point-by-point stepwise GEFA), applied to CESM control run, and CESM dynamical experiments in terms of the **global response in air temperature** to tropical Pacific, Atlantic, and Indian SST EOF1.

	Spat Correl	RMSD	Sign Consistency
Regular GEFA	.73	.63	86%
Stepwise GEFA	.76	.15	91%
Stepwise - Regular	+.03	-76%	+5%

Point-by-point stepwise GEFA yields consistent atmospheric responses to oceanic forcings compared to dynamical experiments.

Point-by-point stepwise GEFA modestly improves the spatial correlation and sign consistency and dramatically reduced the RMSD, leading to more reasonable response field magnitudes.

Evaluation of GEFA

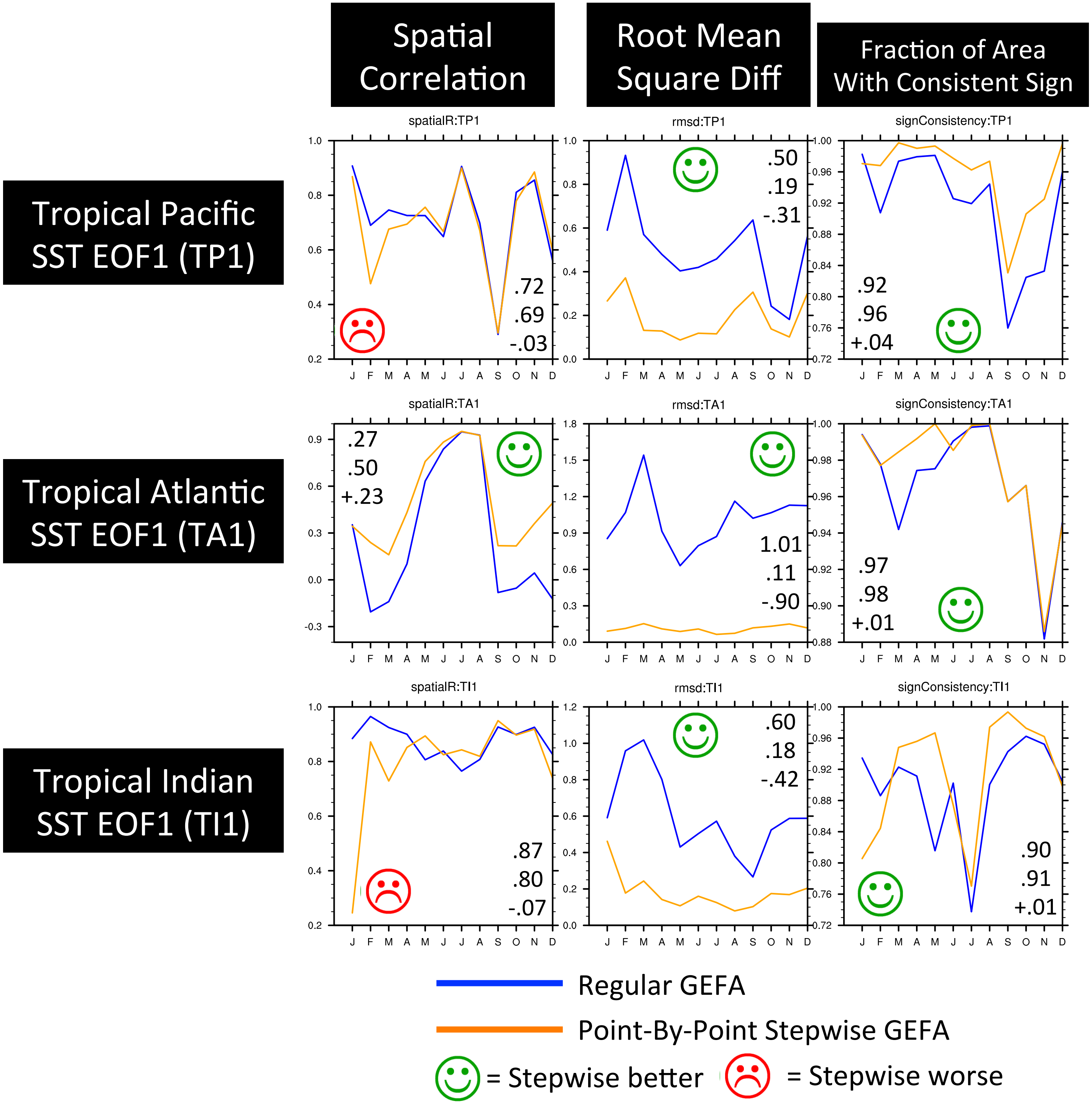

Comparison between statistical GEFA (both regular and point-by-point stepwise GEFA), applied to CESM control run, and CESM dynamical experiments in terms of the **North African response in air temperature** to tropical Pacific, Atlantic, and Indian SST EOF1.

	Spat Correl	RMSD	Sign Consistency
Regular GEFA	.62	.70	93%
Stepwise GEFA	.66	.16	95%
Stepwise - Regular	+.04	-77%	+2%

Evaluation of GEFA

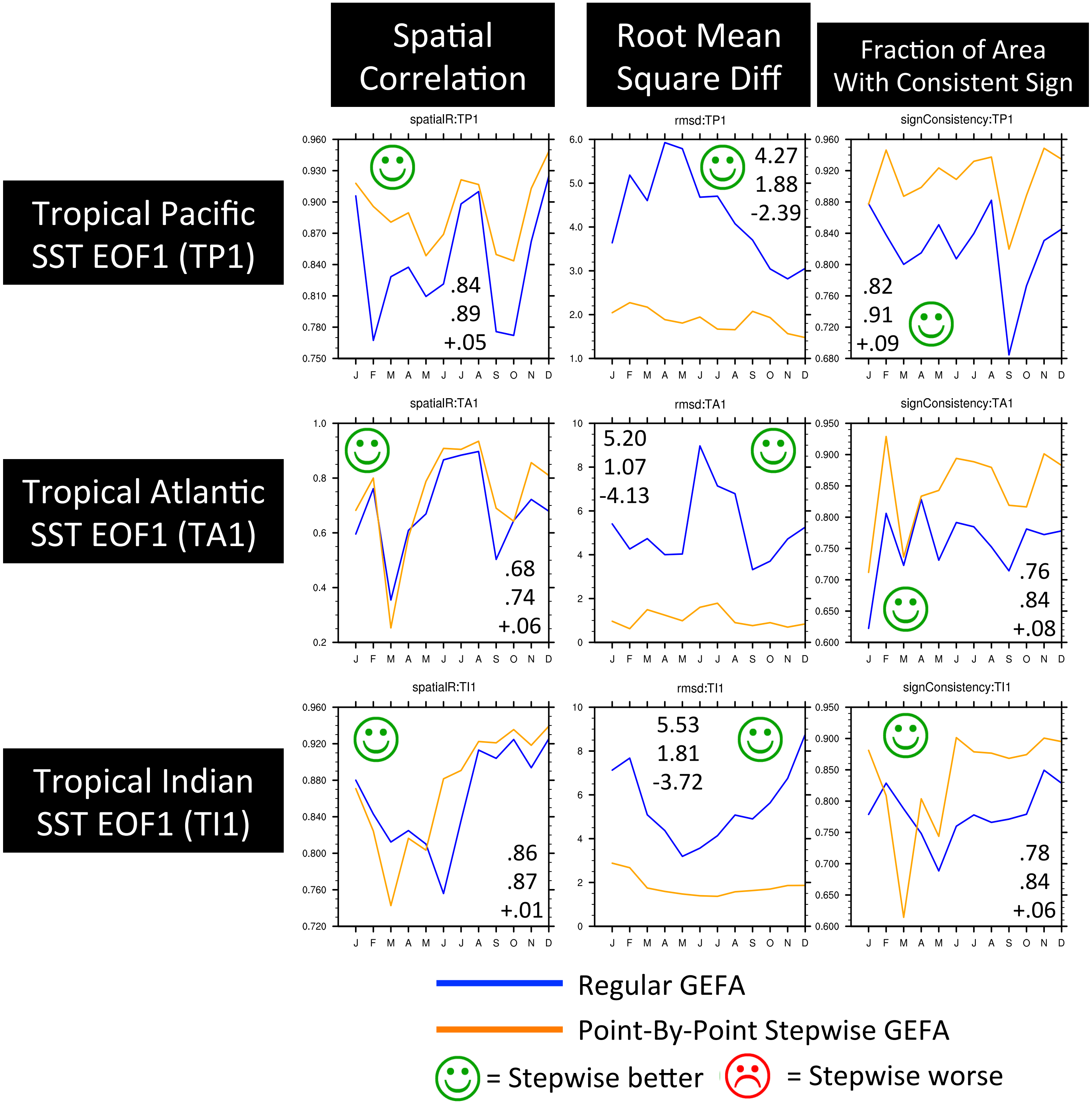

Comparison between statistical GEFA (both regular and point-by-point stepwise GEFA), applied to CESM control run, and CESM dynamical experiments in terms of the **global response in precipitation** to tropical Pacific, Atlantic, and Indian SST EOF1.

	Spat Correl	RMSD	Sign Consistency
Regular GEFA	.79	5.00	79%
Stepwise GEFA	.83	1.59	86%
Stepwise - Regular	+.04	-68%	+7%

Evaluation of GEFA

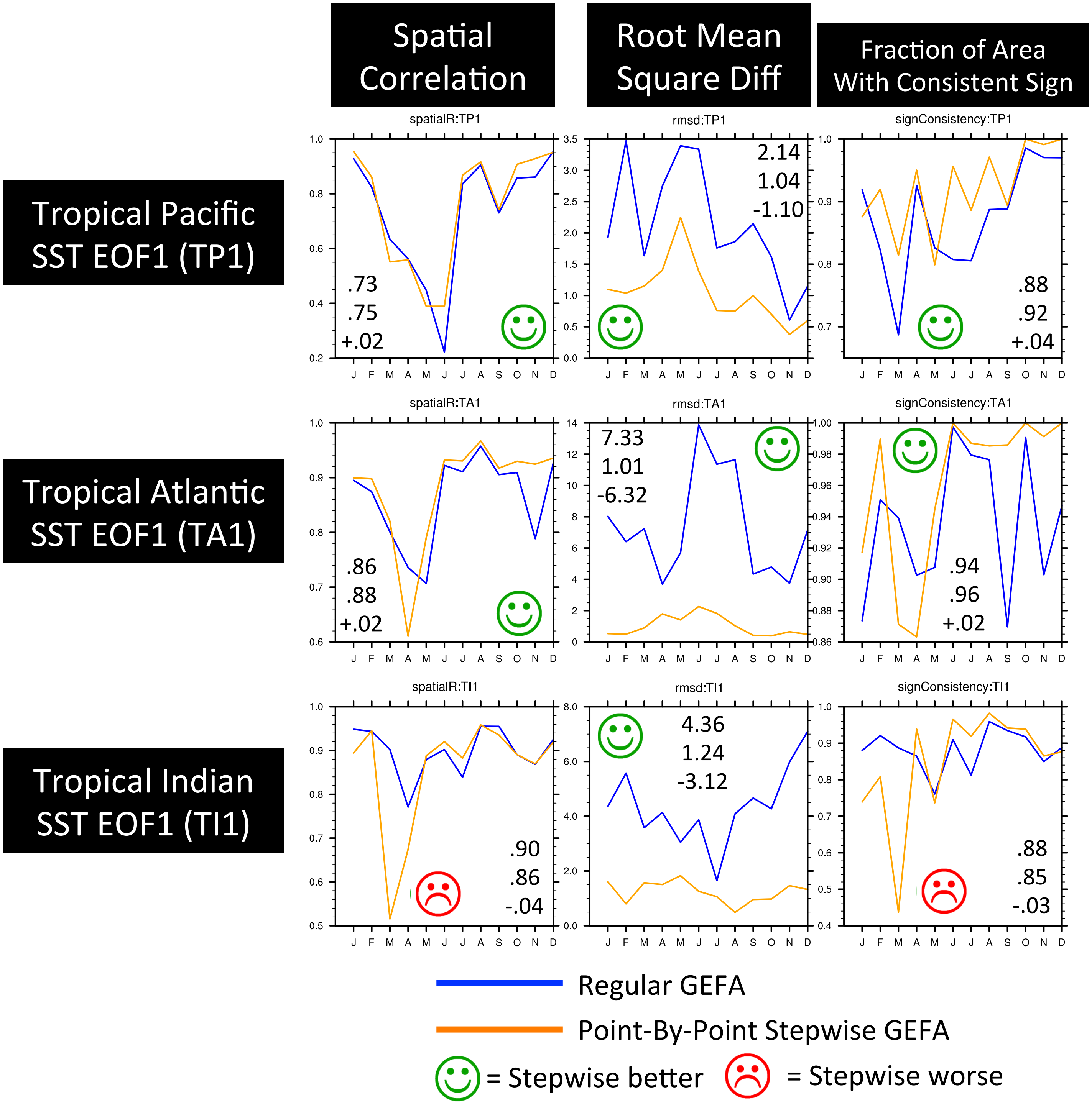

Comparison between statistical GEFA (both regular and point-by-point stepwise GEFA), applied to CESM control run, and CESM dynamical experiments in terms of the **North African response in precipitation** to tropical Pacific, Atlantic, and Indian SST EOF1.

	Spat Correl	RMSD	Sign Consistency
Regular GEFA	.83	4.61	90%
Stepwise GEFA	.83	1.10	91%
Stepwise - Regular	0	-76%	+1%

Primary Oceanic Drivers of North African Climate in CESM

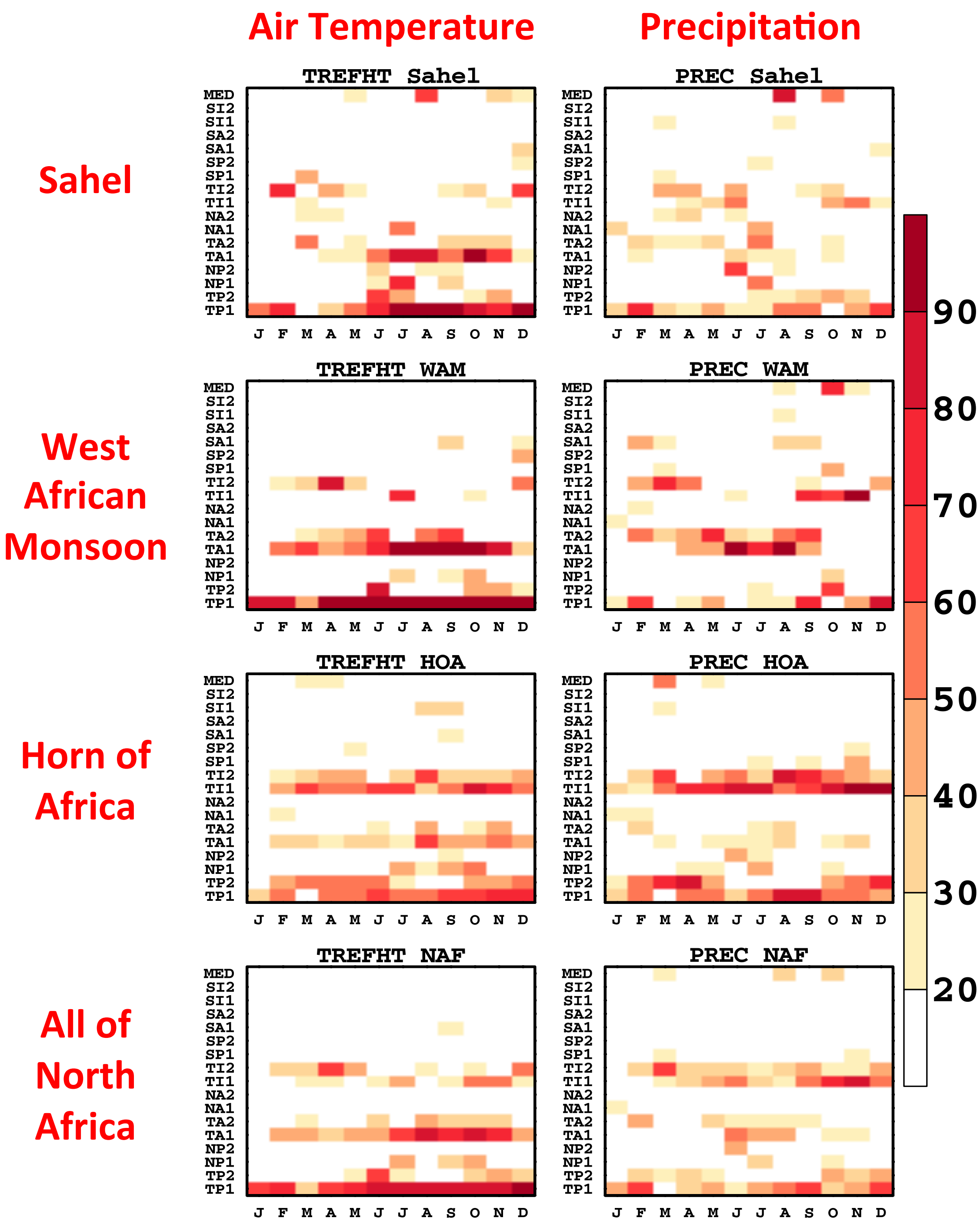

Percentage of study areas with significant (90%+) responses in either air temperature or precipitation, by month, in <u>CESM</u>, according to point-by-point stepwise GEFA

<u>According to GEFA</u>:

The primary oceanic drivers of variability in North African air temperature are the tropical Pacific and tropical Atlantic Oceans in CESM.

The primary oceanic drivers of variability in North African precipitation are the tropical Pacific and tropical Indian Oceans in CESM.

* Tropical ocean basins dominate

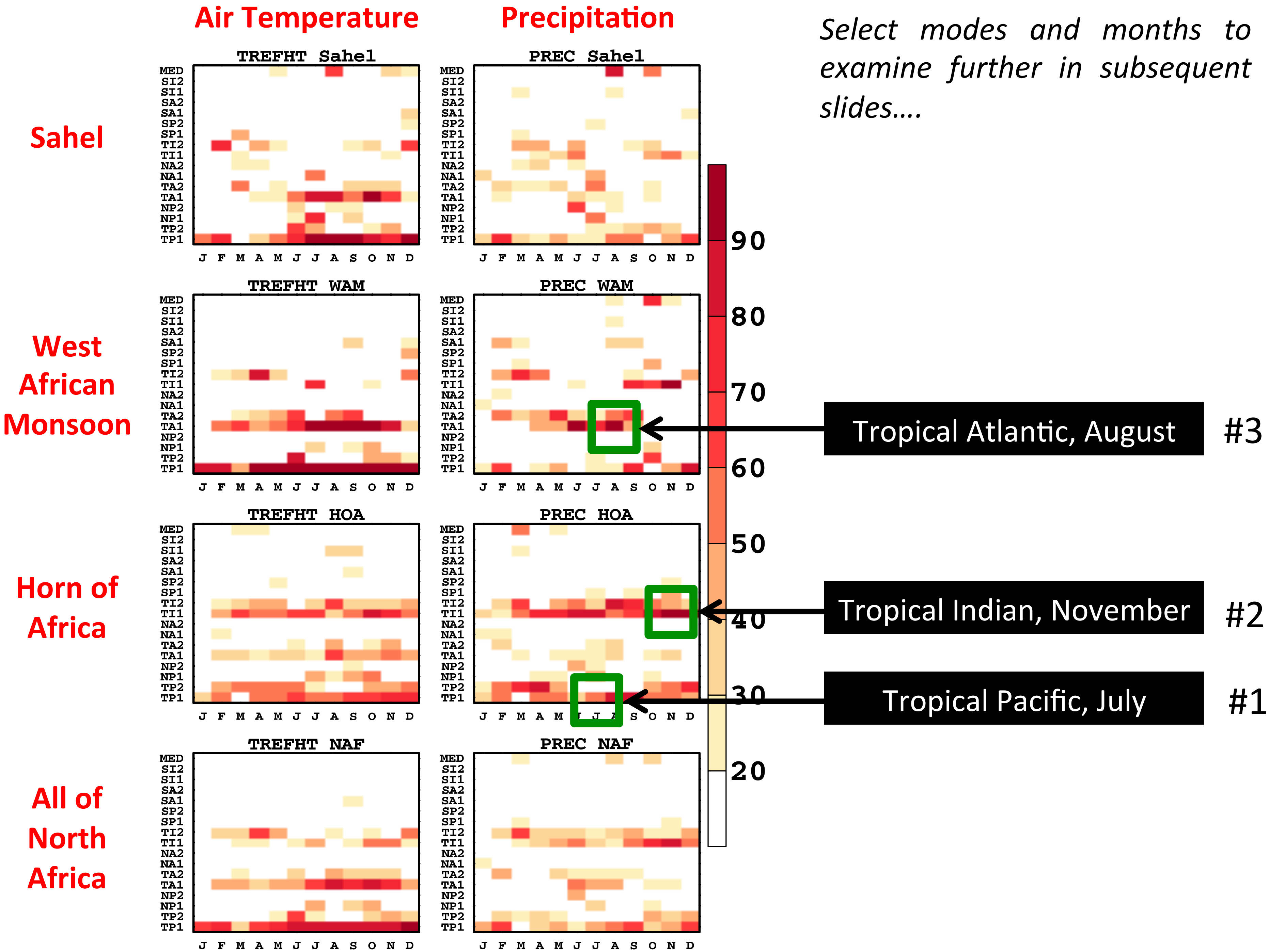

Select modes and months to examine further in subsequent slides….

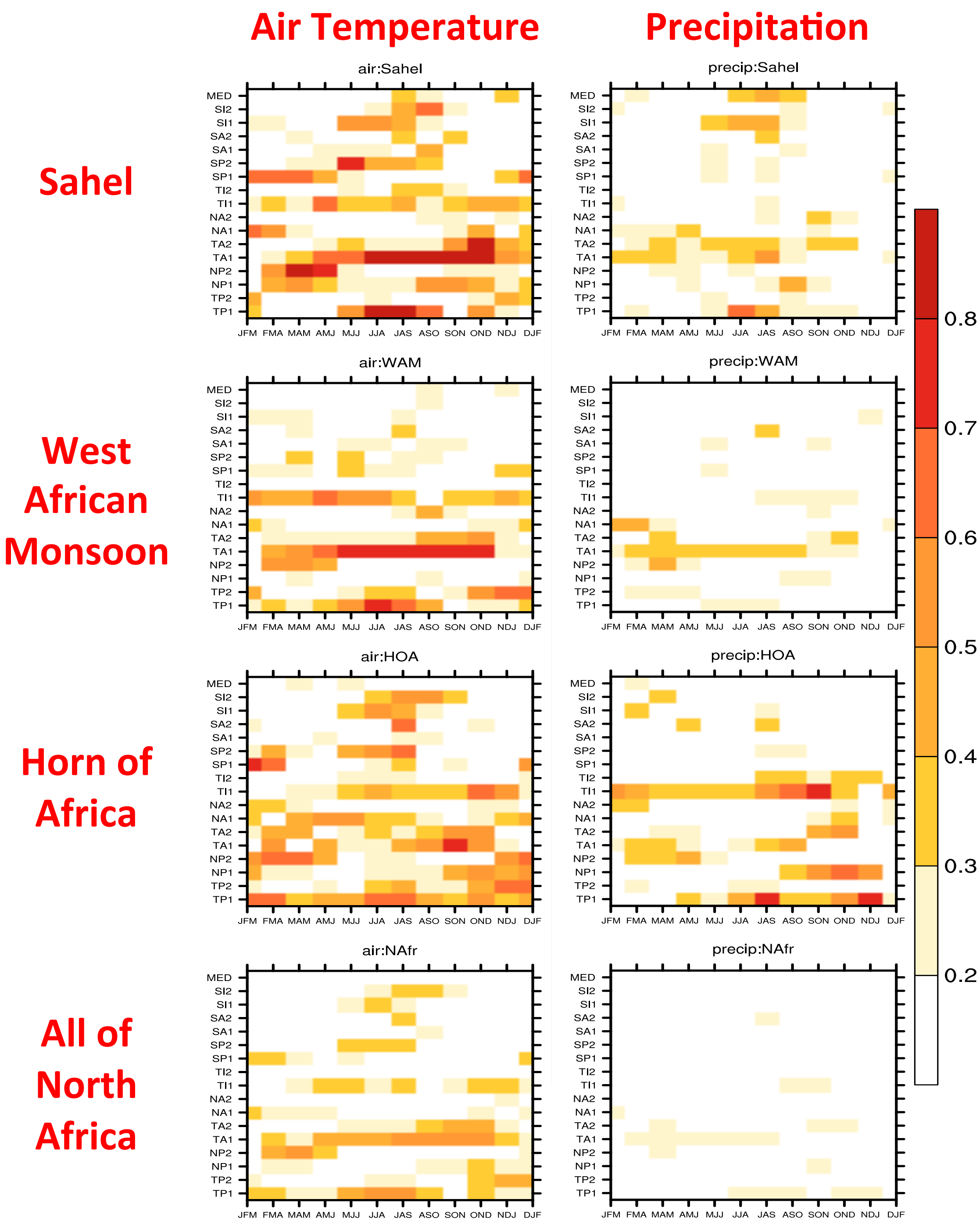

Primary Oceanic Drivers of North African Climate in Observations

Fraction of study areas with significant (90%+) responses in either air temperature or precipitation, by month, in <u>observations</u> (GPCC, 1901-2010), according to point-by-point stepwise GEFA

<u>According to GEFA</u>:

The primary oceanic drivers of variability in North African air temperature are the tropical Pacific and tropical Atlantic Oceans in observations, consistent with CESM.

The primary oceanic drivers of variability in North African precipitation are the tropical Atlantic, Pacific, and Indian, mostly consistent with CESM although with a larger observed contribution from the Atlantic.

* Tropical ocean basins dominate in both observations and CESM

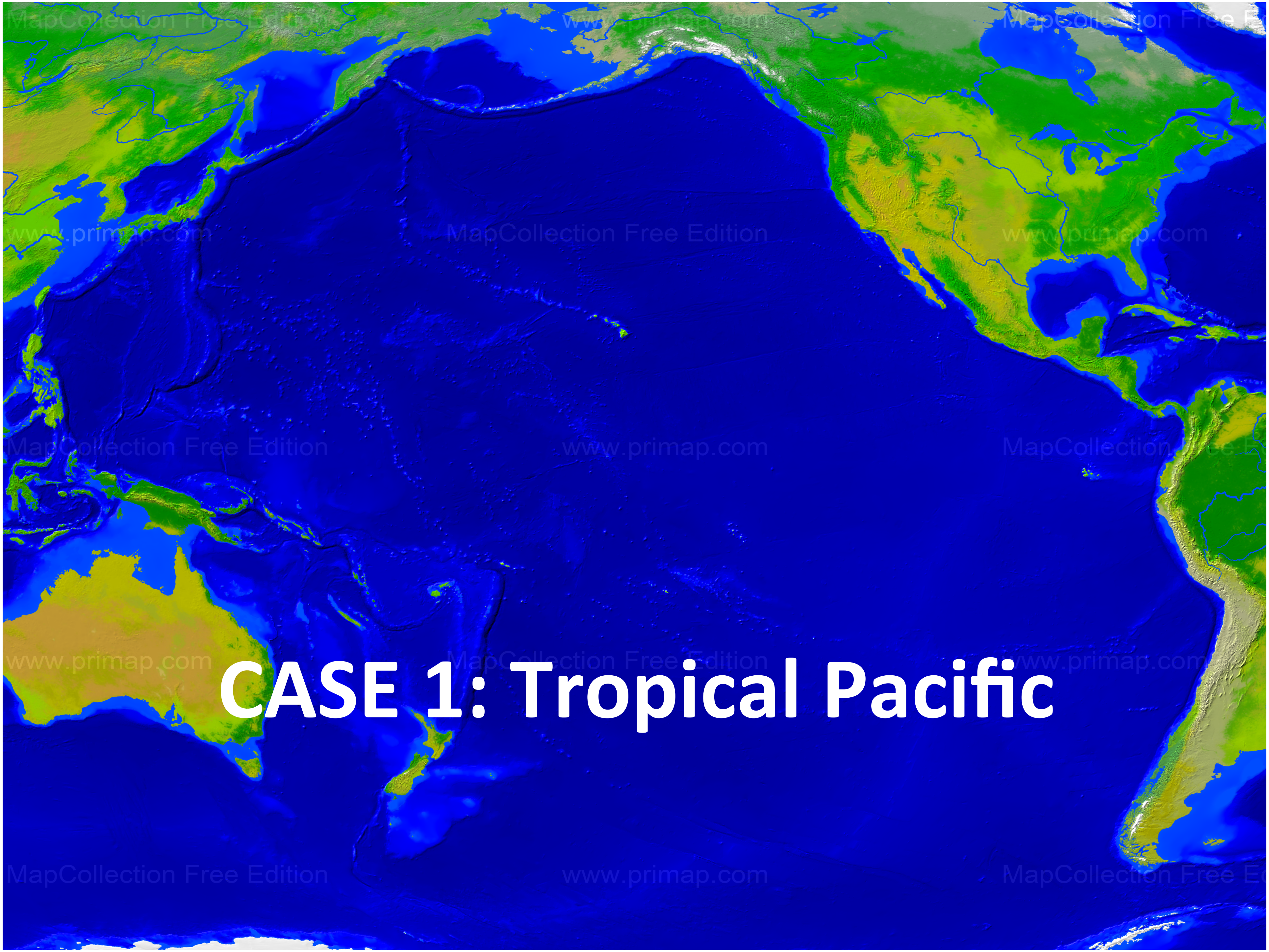

CASE 1: Tropical Pacific

Influence of **Tropical Pacific SST EOF1 in July** on Atmosphere in **CESM,** Based on Point-By-Point Stepwise **GEFA**

Precipitation (cm/month)

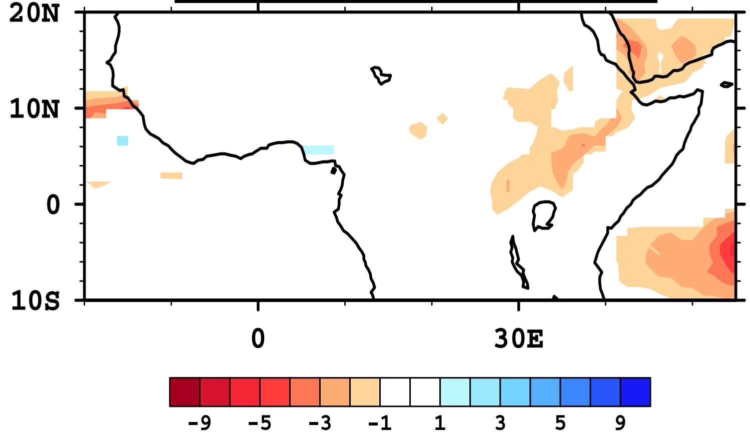

Precipitable Water (shaded, kg/m²), 500-hPa Vertical Motion (Pa/s)

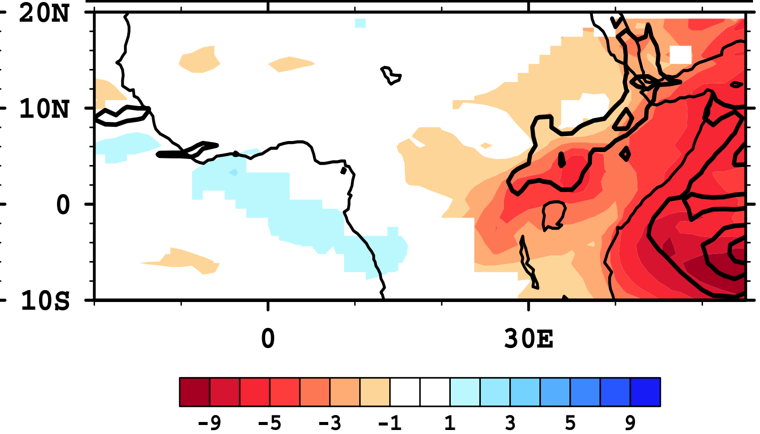

850-hPa Wind Vectors, Heights (shaded, m)

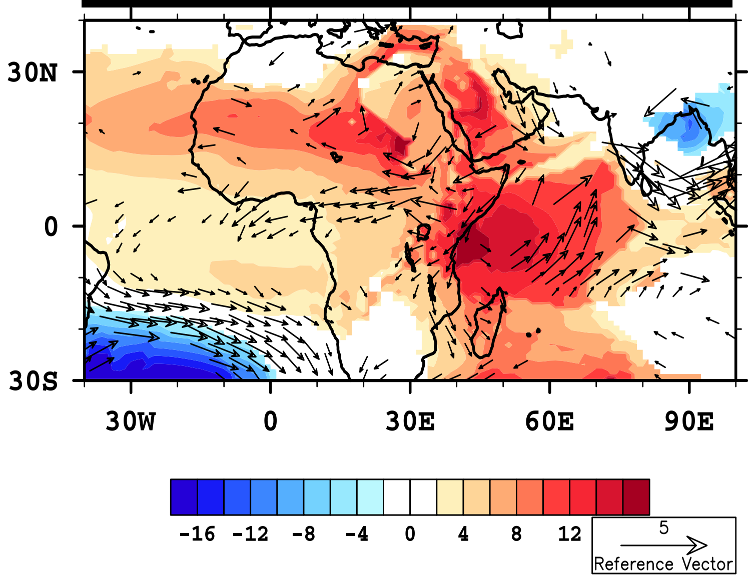

Tropical Pacific July SST EOF1

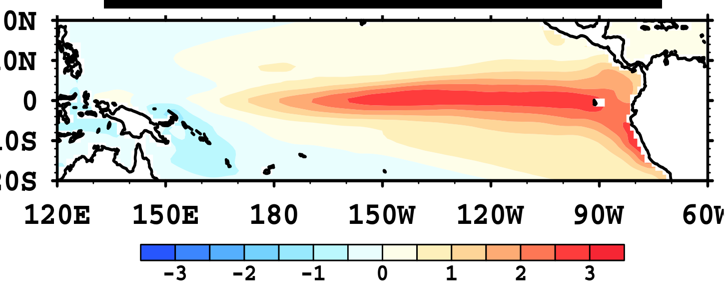

Warm tropical eastern Pacific: Anomalous subsidence (ENSO see-saw pattern), reduced precipitable water / rainfall over Horn of Africa and tropical Indian Ocean in July (dry season)

Influence of Warm Eastern Tropical Pacific in July on Atmosphere in CESM Dynamic Experiments

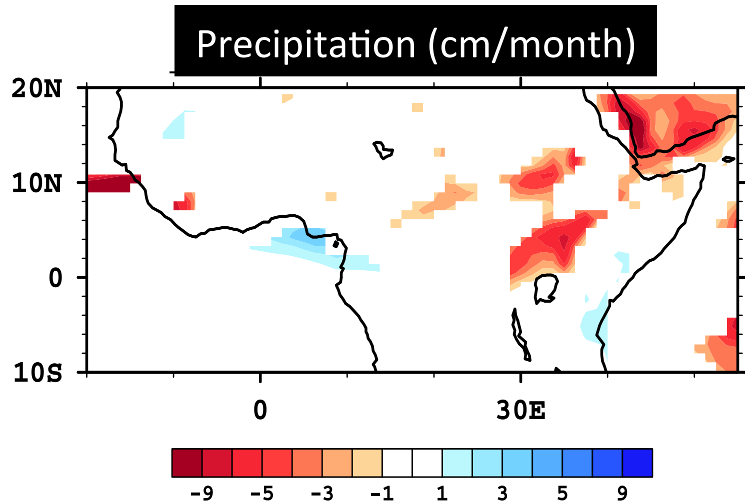

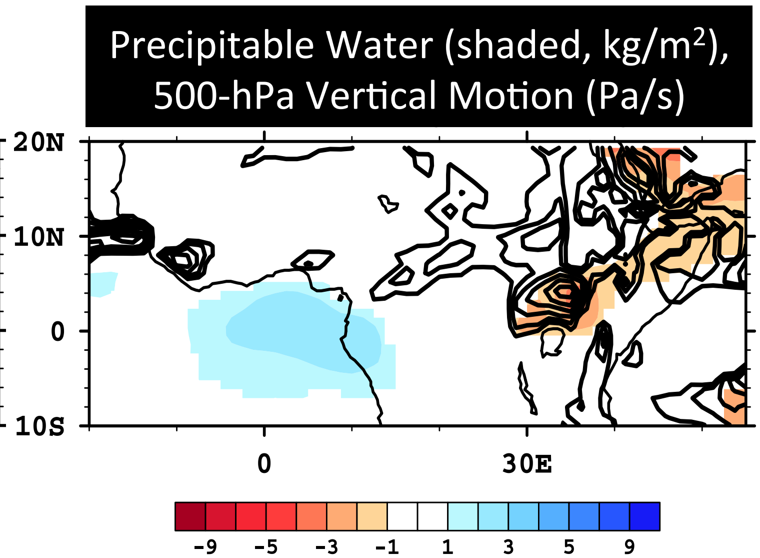

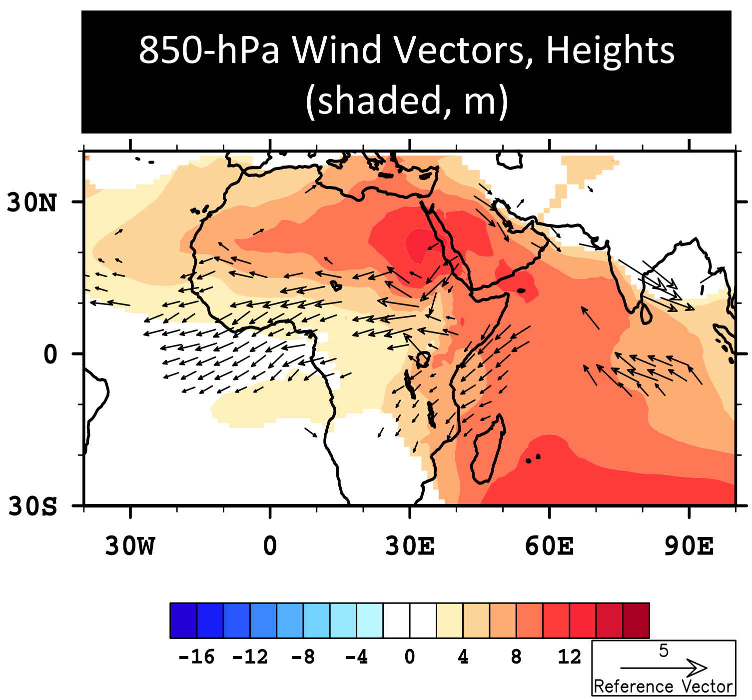

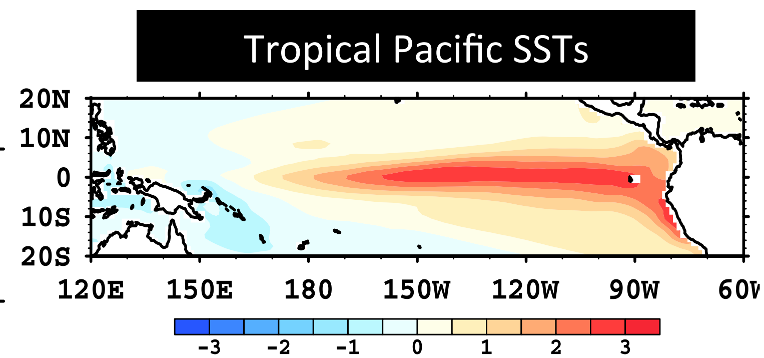

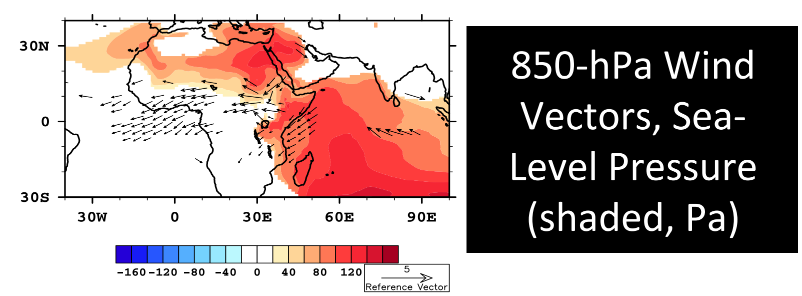

The statistical GEFA method and dynamic experiments in CESM are largely consistent in terms of the impact of tropical Pacific SSTs on North Africa during July, thus validating GEFA.

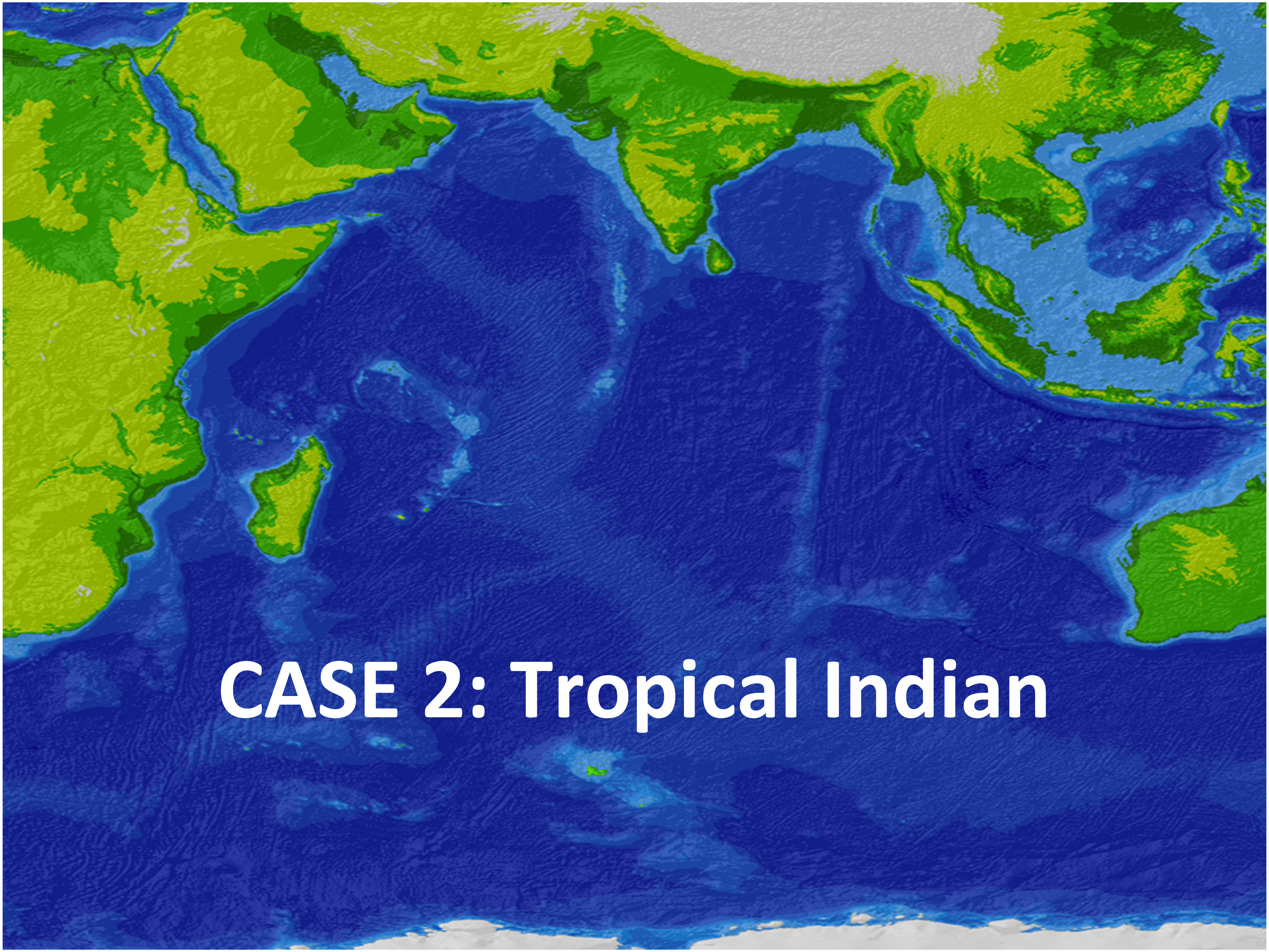
CASE 2: Tropical Indian

Influence of Tropical Indian SST EOF1 in November on Atmosphere in CESM, Based on Point-By-Point Stepwise GEFA

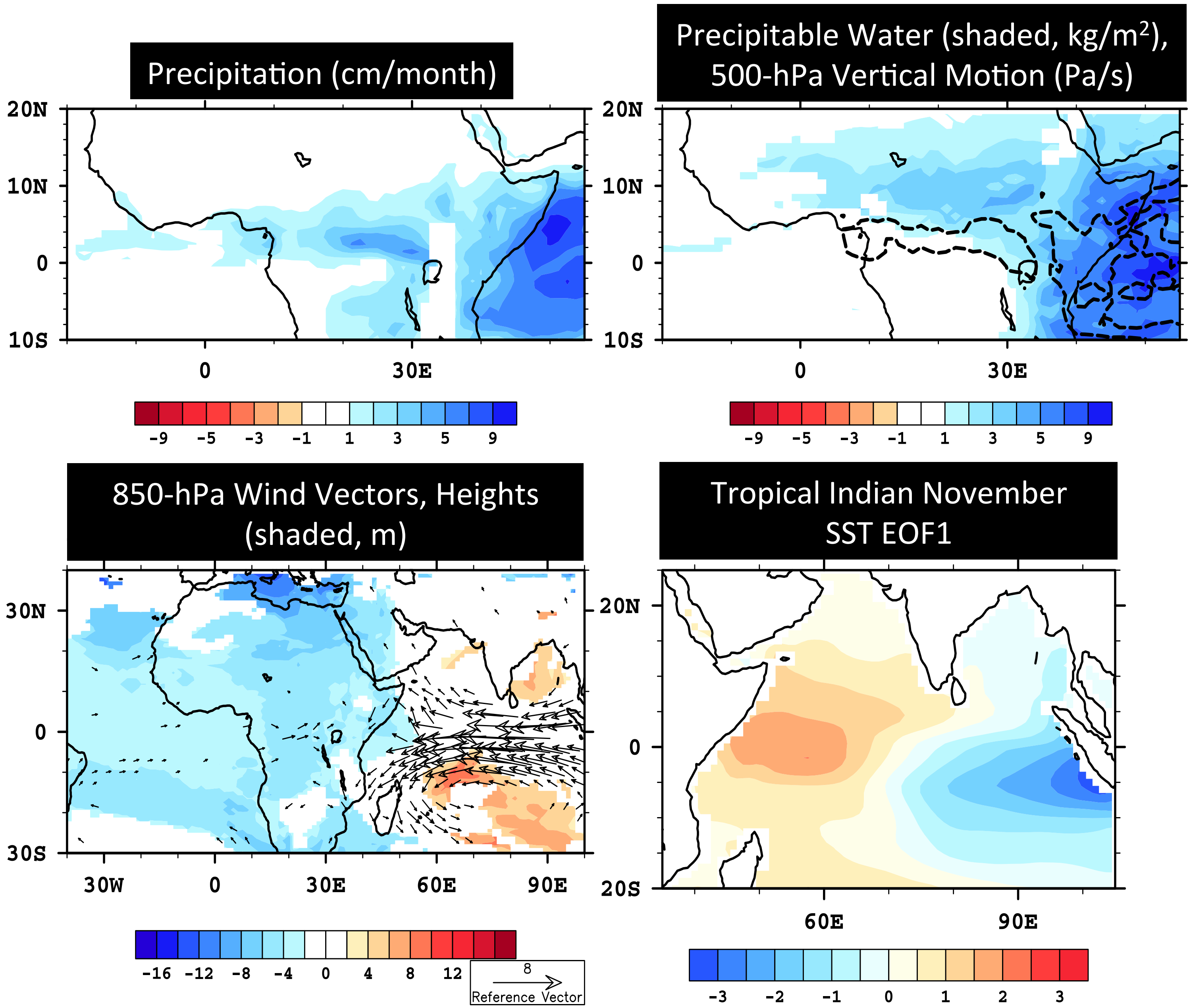

Warm west/cold east tropical Indian: Anomalously easterlies, enhanced moisture advection from Indian Ocean and ascending motion, anomalously wet in Horn of Africa in November (short rains)

Influence of Warm Western Tropical Indian and Cool Eastern Tropical Indian in November on Atmosphere in CESM Dynamic Experiments

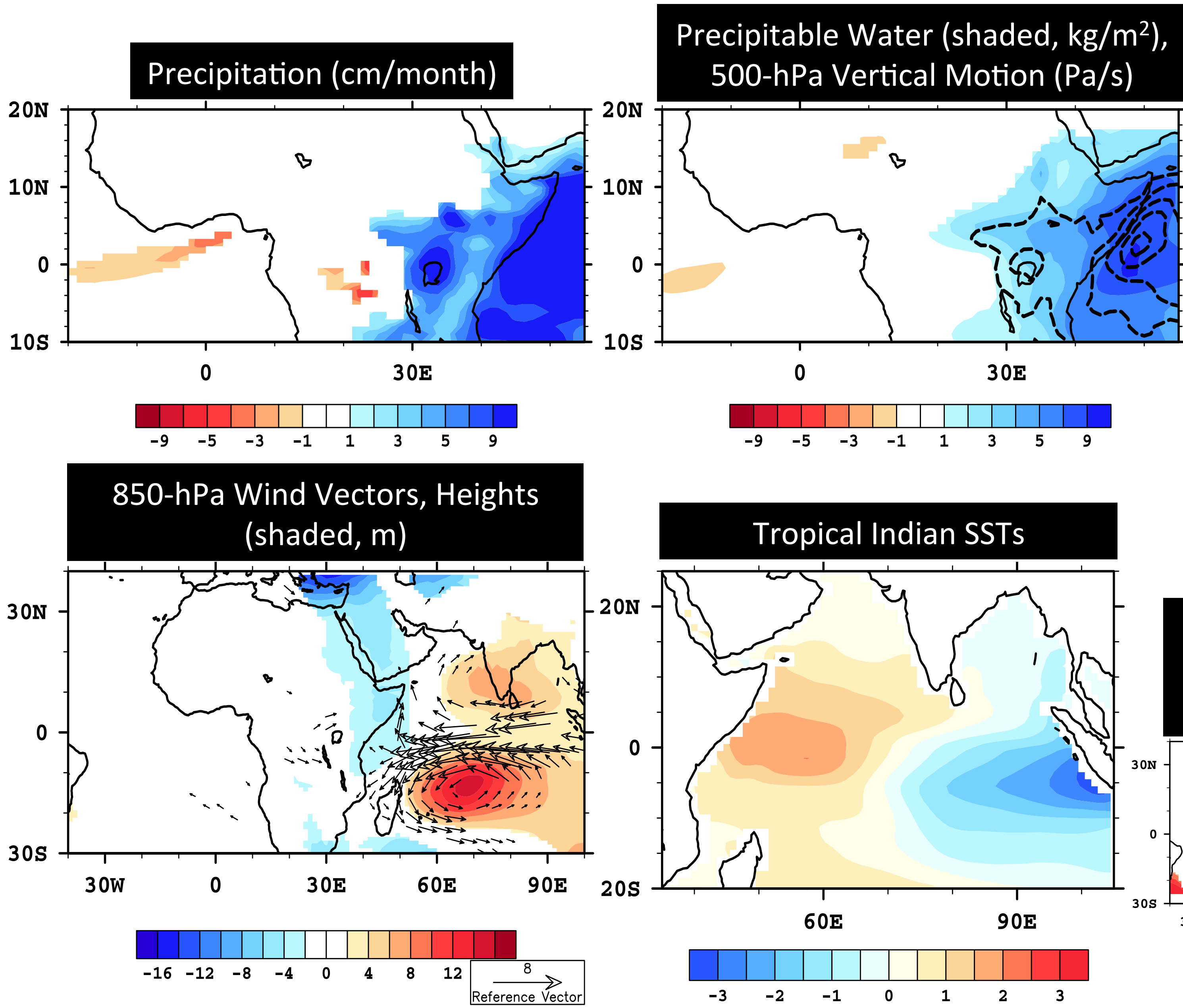

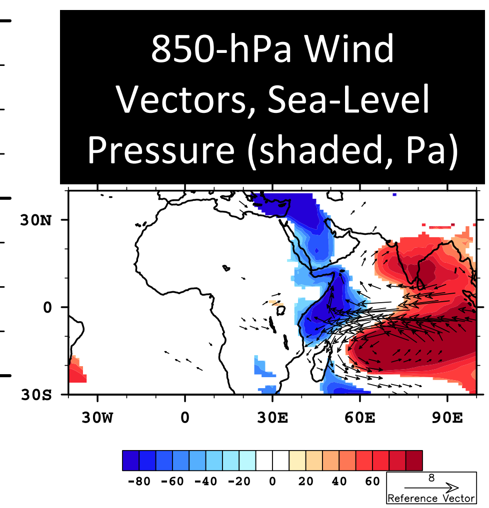

The statistical GEFA method and dynamic experiments in CESM are largely consistent in terms of the impact of tropical Indian SSTs on North Africa during November, thus validating GEFA.

* NOTE THE REVERSED COLOR BAR

Precipitation (cm/month)

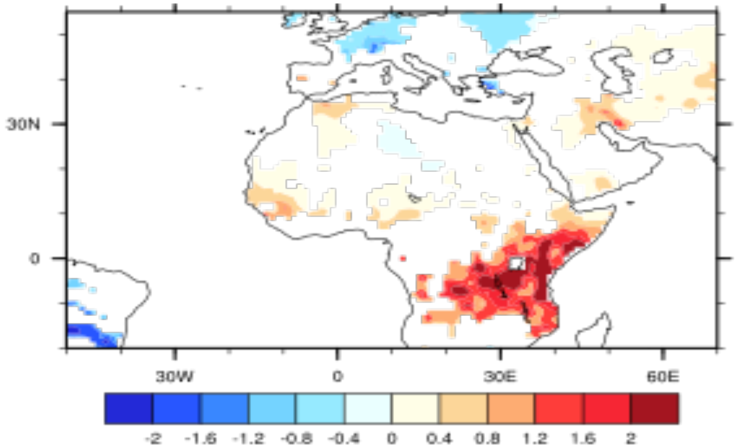

Precipitable Water (shaded, kg/m^2), 500-hPa Vertical Motion (Pa/s)

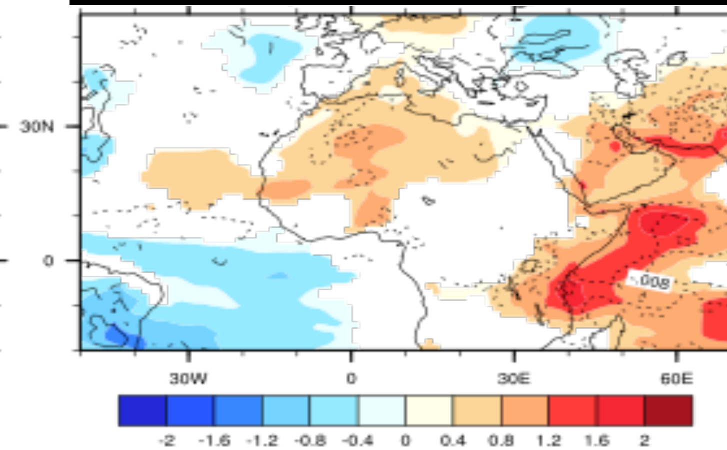

Influence of Tropical Indian SST EOF1 in OND on Atmosphere in Observations, Based on Stepwise GEFA

850-hPa Wind Vectors, Heights (shaded, m)

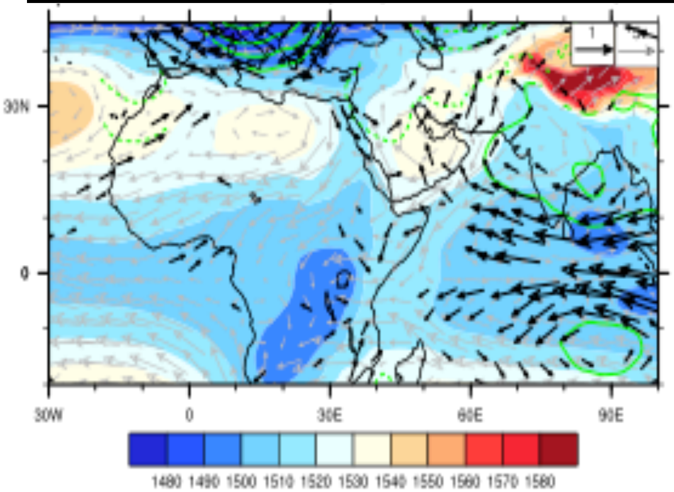

Tropical Indian Oct-Dec SST EOF1

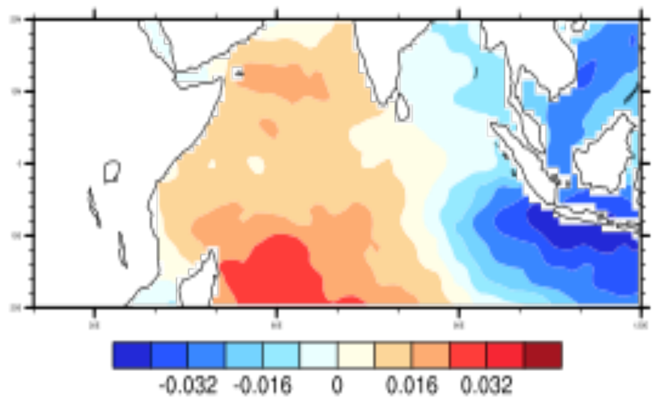

Observations:
GPCC 1901-2010
JRA-55 1958-2011

The observed impacts of TI1 on Africa and associated mechanisms closely match those in CESM.

CASE 3: Tropical Atlantic

Influence of Tropical Atlantic SST EOF1 in August on Atmosphere in CESM, Based on Point-By-Point Stepwise GEFA

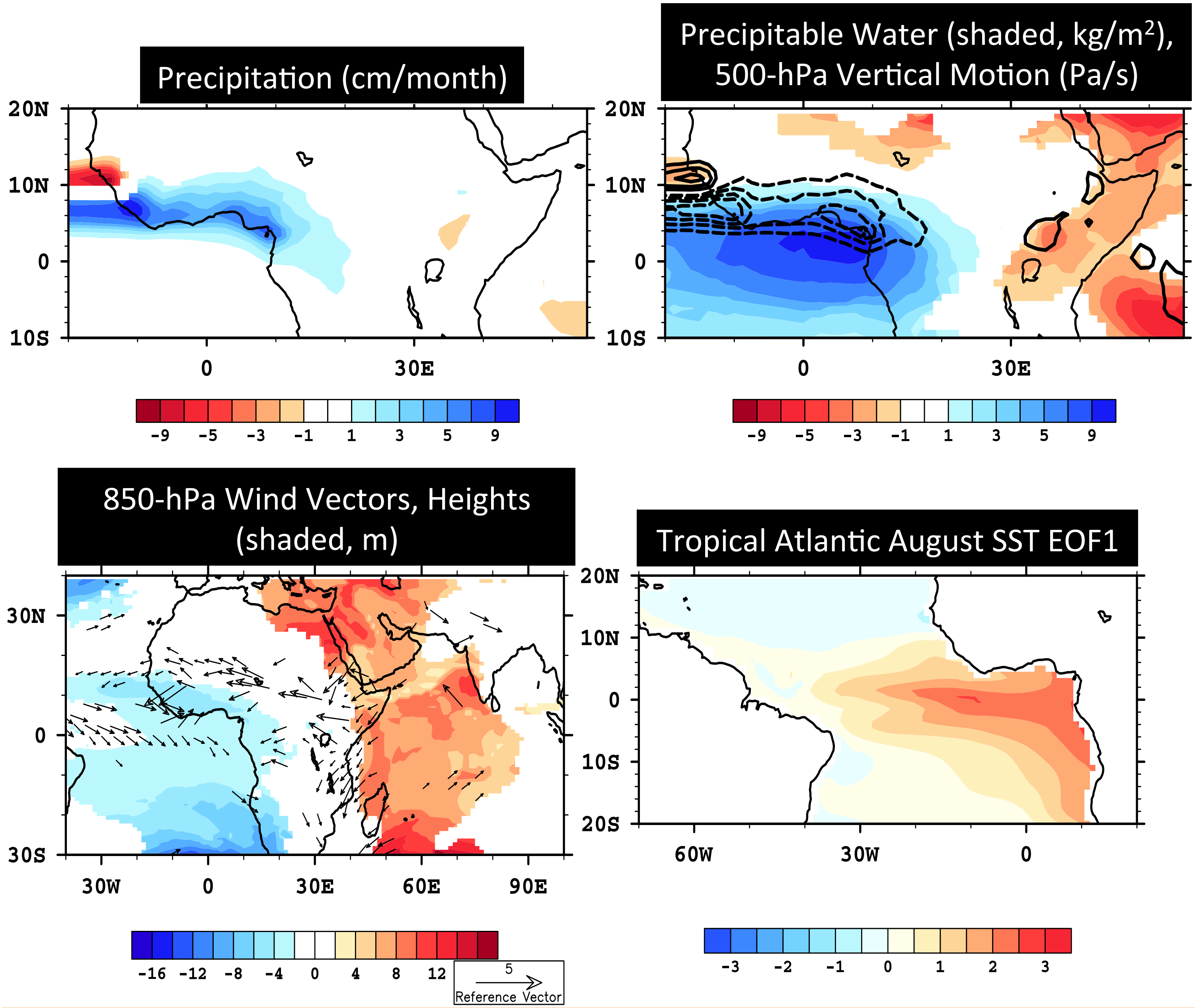

Warm eastern tropical Atlantic: southward shifted ITCZ, enhanced rainfall over the West African monsoon region in August

Influence of Warm Eastern Tropical Atlantic in August on Atmosphere in CESM Dynamic Experiments

Precipitation (cm/month)

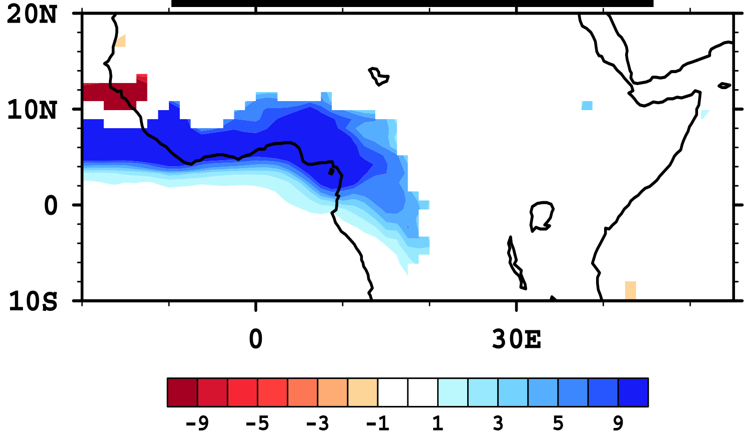

Precipitable Water (shaded, kg/m^2), 500-hPa Vertical Motion (Pa/s)

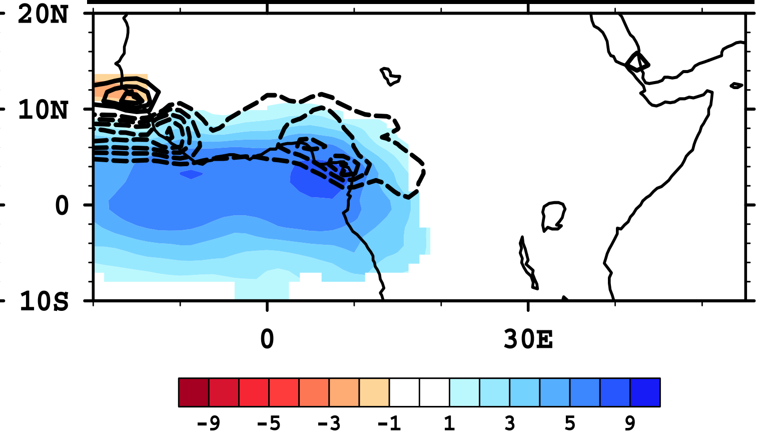

850-hPa Wind Vectors, Heights (shaded, m)

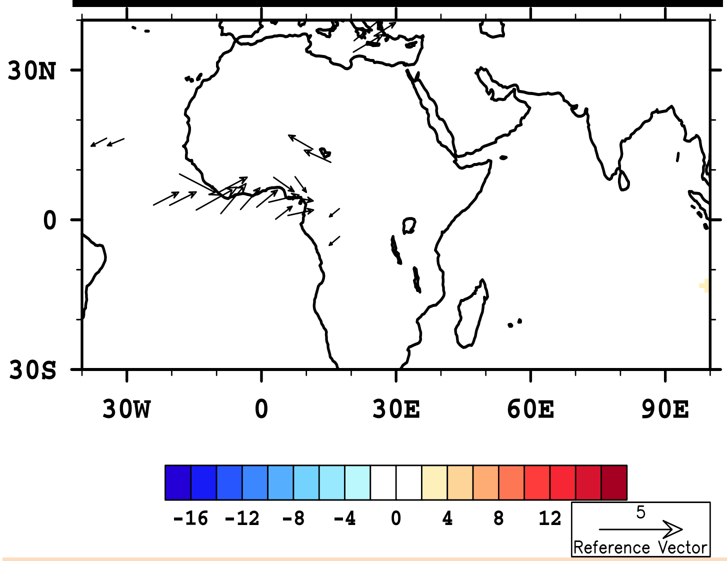

Tropical Atlantic SSTs

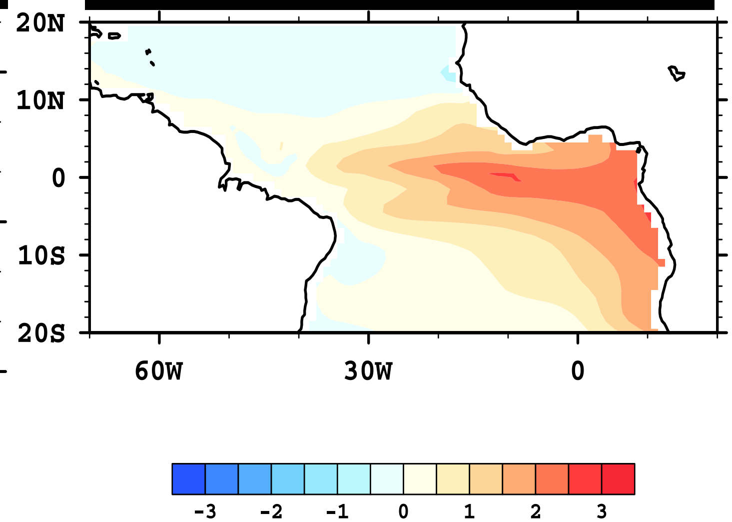

850-hPa Wind Vectors, Sea-Level Pressure (shaded, Pa)

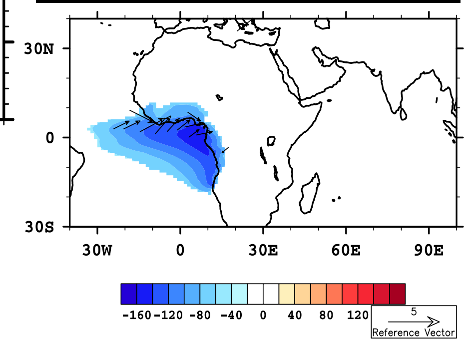

The statistical GEFA method and dynamic experiments in CESM are mostly consistent in terms of the impact of tropical Atlantic SSTs on North Africa during August, thus validating GEFA.

Influence of **Tropical Atlantic SST EOF1 in JAS** on Atmosphere in **Observations**, Based on Stepwise **GEFA**

* NOTE THE REVERSED COLOR BAR

Precipitation (cm/month)

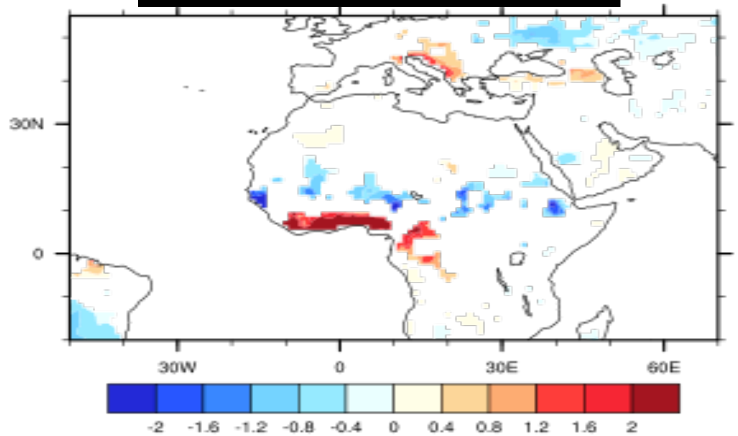

Precipitable Water (shaded, kg/m^2), 500-hPa Vertical Motion (Pa/s)

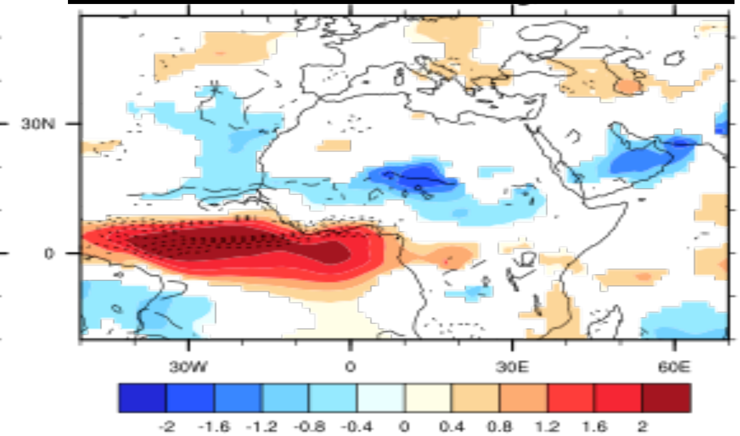

850-hPa Wind Vectors, Heights (shaded, m)

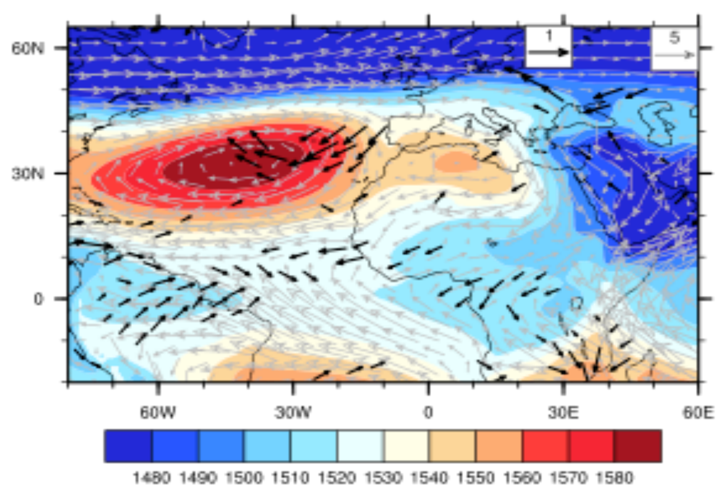

Tropical Atlantic July-Sep SST EOF1

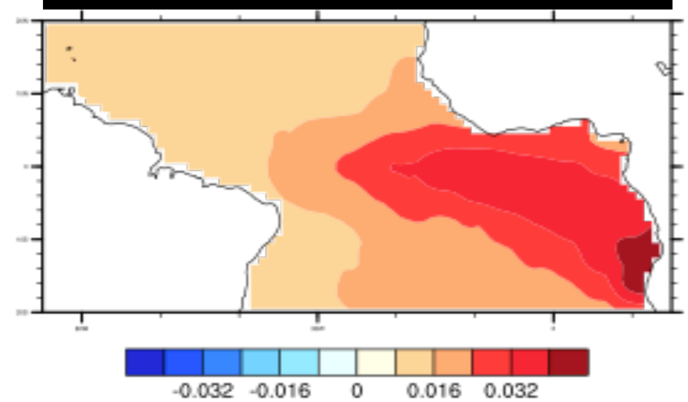

The observations likewise show a shift in the ITCZ in response to TA1, similar to CESM.

Observed Response in Atmospheric Conditions to LAI Anomalies, 1982-2011, According to Stepwise GEFA

Air Temperature | Precipitation

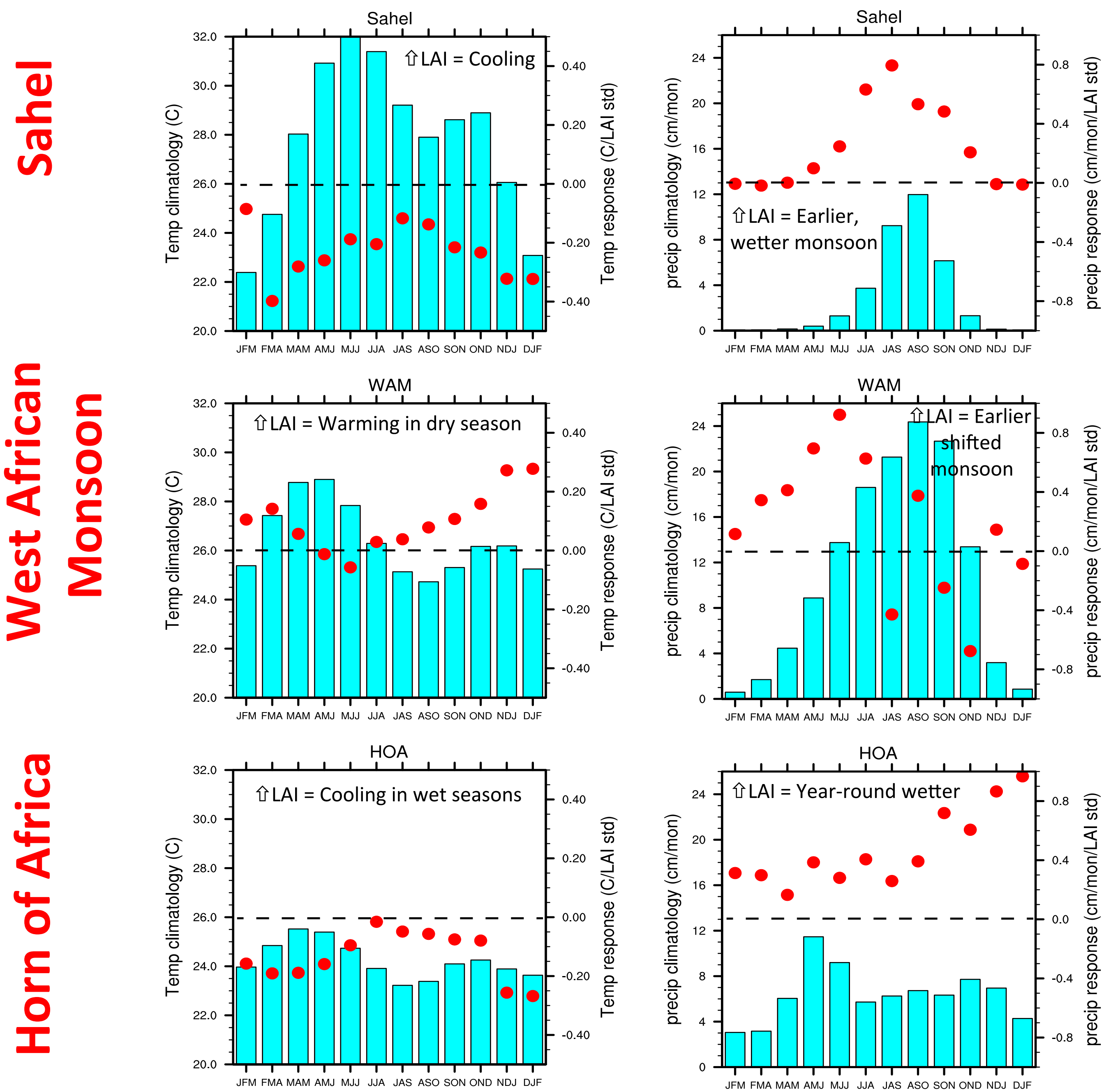

Data Sources:

LAI: GIMMS LAI Boston Univ.

Air Temperature: University of Delaware

Precipitation: GPCP

For semi-arid regions (e.g. Sahel, Horn of Africa), greater LAI leads to more precipitation and lower air temperatures. About 50% of the precipitation response seems to be linked to moisture recycling through greater ET.

Greater LAI seems to support an earlier shifted West African monsoon. That region does not seem to benefit from the enhanced ET, as the PWTR response is small.

Evapotranspiration | Precipitable Water

Observed Response in Atmospheric Conditions to LAI Anomalies, 1982-2011, According to Stepwise GEFA

Sahel

West African Monsoon

Horn of Africa

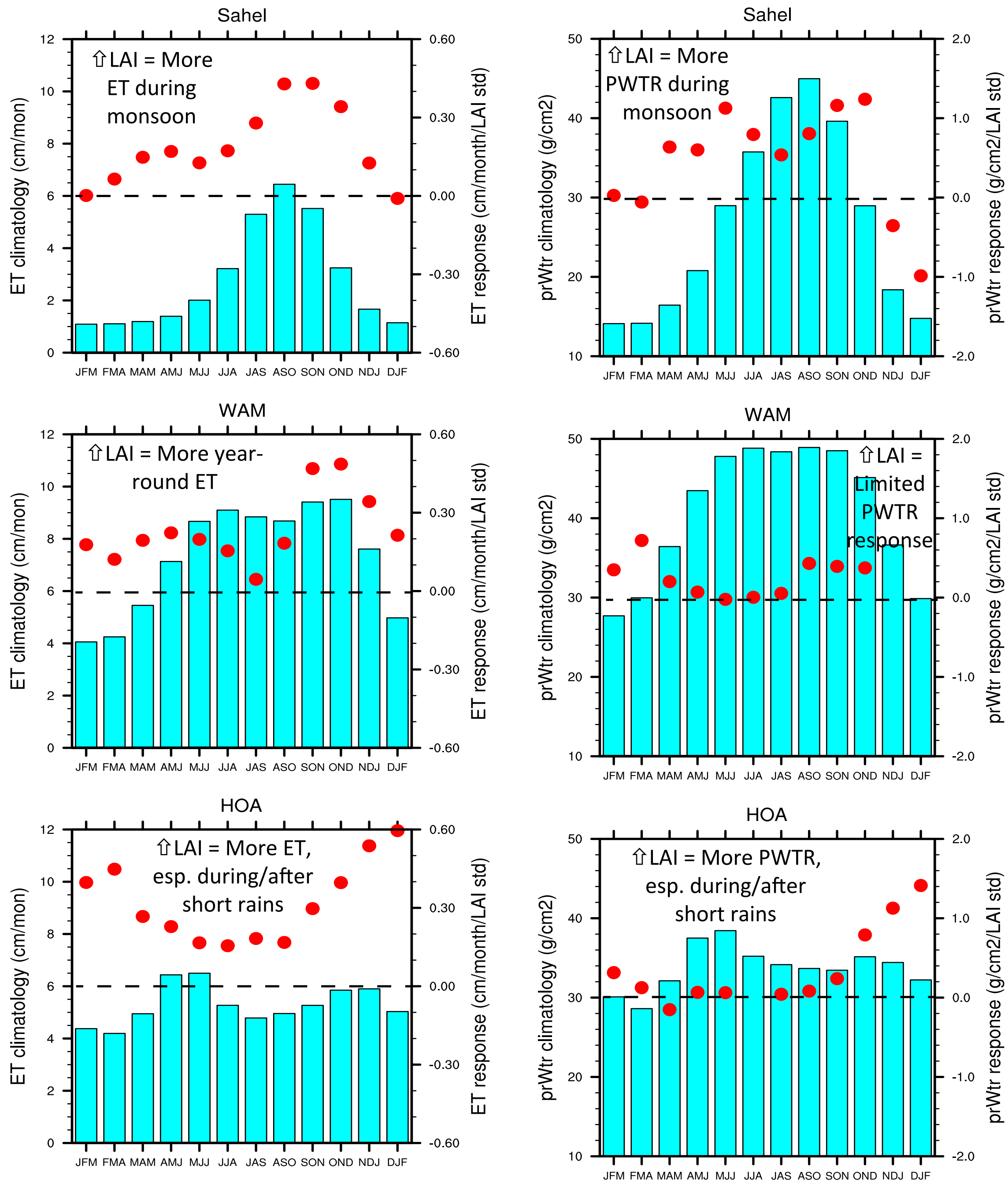

Data Sources:

LAI: GIMMS LAI Boston Univ.

Evapotranspiration: Jiafu Mao's merged product

Precipitable Water: ERA Interim

* Will consider a spectrum of observational datasets to produce a distribution of feedback estimates and assess robustness

Conclusions

Our project aims to decompose the observed oceanic and terrestrial drivers of regional climate across North Africa, with benefits to seasonal prediction and model evaluation/improvement.

We have initially demonstrated the reliability of GEFA at quantifying the atmospheric response across North Africa to oceanic forcings. We have shown increased accuracy with longer time records and clear improvements in feedback estimates when applying the stepwise GEFA approach.

Future work will consist of:

(1) Validating GEFA in terms of the impacts of LAI variability on atmospheric conditions within CESM through further dynamic experiments,

(2) Quantifying the impact of LAI variability in observations,

(3) Assessing the robustness of observed response fields to oceanic and terrestrial drivers by considering a spectrum of available observational datasets.

(4) Evaluating the CMIP5 models' capability of simulating the oceanic and terrestrial drivers of North African regional climate compared to the GEFA-based observed benchmark, and

(5) Examining changes in the relative importance and impacts of these drivers under future climate change within CMIP5 models.